Article

Efficient Removal of Organic Dye from Aqueous Solution Using Hierarchical Zeolite-Based Biomembrane: Isotherm, Kinetics, Thermodynamics and Recycling Studies

Sabarish Radoor [1,*], Jasila Karayil [2], Aswathy Jayakumar [1], Jaewoo Lee [3,4], Debabrata Nandi [1], Jyotishkumar Parameswaranpillai [5], Bishweshwar Pant [6,7,*] and Suchart Siengchin [1,8,*]

[1] Materials and Production Engineering, The Sirindhorn International Thai-German Graduate School of Engineering (TGGS), King Mongkut's University of Technology North Bangkok, Bangkok 10800, Thailand
[2] Government Women's Polytechnic College, Calicut 673009, India
[3] Department of Polymer-Nano Science and Technology, Jeonbuk National University, 567 Baekje-daero, Deokjin-gu, Jeonju-si 54896, Korea
[4] Department of Bionanotechnology and Bioconvergence Engineering, Jeonbuk National University, 567 Baekje-daero, Deokjin-gu, Jeonju-si 54896, Korea
[5] Department of Science, Alliance University, Bengaluru 562106, India
[6] Carbon Composite Energy Nanomaterials Research Center, Woosuk University, Wanju 55338, Korea
[7] Woosuk Institute of Smart Convergence Life Care (WSCLC), Woosuk University, Chonbuk, Wanju 55338, Korea
[8] Institute of Plant and Wood Chemistry, Technische Universität Dresden, Pienner Str. 19, 01737 Tharandt, Germany
[*] Correspondence: sabarishchem@gmail.com (S.R.); bisup@woosuk.ac.kr (B.P.); suchart.s.pe@tggs-bangkok.org (S.S.)

Abstract: Bio adsorbents have received tremendous attention due to their eco-friendly, cheap and non-toxic nature. Recently, bio-adsorbent-based membranes have been frequently employed for water treatment. The work reports the preparation of a novel adsorbent membrane from hierarchical zeolite, polyvinyl alcohol, carboxymethyl cellulose and agar. The fabricated membrane was characterized spectroscopically and microscopically with several techniques such as XRD, UTM, TGA, optical microscopy and FT-IR, as well as contact-angle studies. The result showed that the hierarchical-zeolite-loaded membrane is superior in terms of thermal stability, mechanical properties and surface roughness. The fabricated membrane was investigated for its efficiency in the removal of Congo red dye in aqueous conditions. The influence of pH, temperature, contact period and the initial concentration of dye and zeolite loading on the adsorption process are also explored. The adsorption results highlighted the maximum sorption property of Congo red on agar/zeolite/carboxymethyl cellulose/polymer biomembrane was found to be higher (15.30 mg/g) than that of zeolite powder (6.4 mg/g). The adsorption isotherms and kinetic parameters were investigated via Langmuir, Freundlich and pseudo-first order, pseudo-second order and the intraparticle diffusion model, respectively. The adsorption isotherms fitted well for both considered isotherms, whereas pseudo-second order fitted well for kinetics. The thermodynamic parameter, ΔG at 303 K, 313 K and 323 K was −9.12, −3.16 and −0.49 KJ/mol, respectively. The work further explores the antibacterial efficacy of the prepared membrane and its reusability.

Keywords: carboxymethyl cellulose; agar; congo red; ZSM-5 zeolite; bio adsorbent

1. Introduction

Water is an essential resource for the existence of life on planet Earth. However, over the past few decades a large amount of wastewater has been released into the freshwater bodies, thus making it unusable for living beings [1–3]. Anthropogenic activities are mainly responsible for water pollution [4,5]. Municipal waste, industrial waste, agricultural

effluents and radioactive wastes are some of the main sources of water pollution [6,7]. Natural phenomena (volcanos, earthquakes, etc.) also degrade the quality of fresh water. In the last few decades, water pollution has been escalating at an alarming pace and poses a serious threat to the environment [8–10]. One of the major pollutants in industrial effluents are dyes. Synthetic dyes are toxic, non-biodegradable, carcinogenic and mutagenic materials which cause serious health problems to both humans and aquatic systems [11,12]. The high stability of dyes is responsible for their strong resistance towards aerobic digestion, light, heat and oxidizing agents. Therefore, the discharge of dyes from aqueous solution is one of the toughest challenges faced in recent years. The development of an efficient, biodegradable and inexpensive route for the removal of effluents from sewerage is most challenging job. Some of the commonly used techniques for treating dye-laden water are coagulation, precipitation, filtration, reverse osmosis, photo degradation, ion exchange, electrochemical techniques and adsorption [13,14]. Because of its high efficiency and high regeneration capacity, the adsorption technique is considered the prevailing method for dye-removal studie s [15,16]. Along with activated carbon, several other adsorbents, such as agricultural wastes, clay, metal oxides, fly ash, cellulose, wood, rice husk and zeolites, have been investigated for water treatment [17–22]. In recent years, a variety of adsorbents, such as composite adsorbents and multi-functional materials have been used for dye-removal studies [23].

Zeolite is one of the naturally available aluminosilicate materials. Owing to its greater surface area and porous properties, it is highly explored as an adsorbent [24,25]. Conventional zeolites have microporous structure (pore size < 2 nm), and therefore are not suitable for the adsorption of high-molecular-size dye molecules [26,27]. This problem could be overcome by the utilization of hierarchical zeolite which contains micro-, meso- and macropores [28]. Many reports are available on the use of micro/macropore zeolite for the removal of contaminants from wastewater. In recent years, zeolite-based composite membranes have become an attractive alternative to the conventional adsorbent method. The benefits of using membrane technology are its high regeneration capacity, low time consumption and high adsorption efficiency [29,30].

There are ample reports on zeolite-based polymer membranes for water-treatment applications [25,31]. To improve its dye-adsorption performance, zeolite has often used in combination with polymers or other nanomaterials [32,33]. A high percentage of dye removal (96%) was noted for poly(vinylidene fluoride) PVDP/zeolite membrane [34]. Meanwhile, the complete elimination of a toxic dye, methylene blue (MB), from water was achieved by a zeolite/PVA/chitosan electro-spun nanofibrous composite. High dye-removal efficacy along with good mechanical and reusable properties make it suitable candidate for industrial applications [35]. Baheri et al. [36] studied the MB adsorption process of a 4A-zeolite/polyvinyl alcohol mixed-matrix membrane. Their studies revealed that the zeolite percentage has positive effect on the adsorption process, which is in agreement with the previous report [37]. The higher adsorption of 9.18 mg/g was noted for 20 wt% of zeolites. Abukhadra and co-worker [38] applied three different types of natural zeolite (clinoptilolite, phillipsite and heulandite) for efficient dye removal (safranin-T) from waste streams. The comparison of their adsorption capacity revealed that heulandite has the highest safranin uptake, followed by phillipsite and clinoptilolite. In the case of heulandite, the process equilibrium was attained after 240 min. The pH-dependent adsorption was also noted, and the alkaline medium was found to be the most suitable for safranin removal using zeolite. Zeolite/algae composite (ZAS) was proposed as a substitute adsorber for CR elimination from contaminated water. Even at a low adsorbent dosage, it displayed 98% removal efficiency [39]. A highly efficient and fast Congo red adsorption was achieved using a ZnO functional zeolite. Complete dye removal was achieved within 20 min. Dryaz et al. [40] reported that a Padina gymnospora/zeolite nanocomposite has a sufficient number of hot spots available for CR adsorption. Maroofi et al. [41] developed zeolitic imidazolate incorporated-polyvinylpyrrolidone-polyethersulfone composite membranes for malachite green (MG) dye removal. The high MG removal efficiency (99.6%) of the composite was

ascribed to the electrostatic interactions between the MG dye and composite, which had positive and negative charges, respectively. Recently, our group fabricated a series of zeolite-based composites for various dye-removal studies [20,42]. Our studies revealed that zeolite played a crucial role in the adsorption property of the polymer membrane.

Carboxymethyl cellulose (CMC) is a naturally occurring anionic polymer which is explored in the water-treatment process especially for the removal of charged dyes. The anionic functional group of the CMC increases its affinity for cationic dyes [43]. The dye-adsorption properties of CMC could be further enhanced by grafting or if used in combination with graphene oxide, polymers, chitosan, etc. [44]. CMC/k-carrageenan (KC)/activated montmorillonite (AMMT) composite is highly effective at removing cationic dye. The dye was removed almost completely within 120 min of contact time [45]. The electrostatic attraction between the copper oxide (CuO)-CMC composite and the MB is stated as the reason for the dye-adsorption ability of the CuO-CMC composite. Cellulose-based graphene oxide hydrogels are reported to be a potential aspirant for the removal of acid blue-133 from aqueous system [46].

Agar is a polysaccharide extracted from the cell walls of red algae. Agar is used in food industry as an emulsifying, gelling and stabilizing agent. Agar is composed of 70% agarose, which is a linear polysaccharide, and 30% agaropectin which is a branched polysaccharide. Agar and agar-based composites are reported to have the ability to remove various contaminants from water. For instance, the usage of agar for the successful removal of MB is reported. The mechanism of dye adsorption is proposed as being electrostatic interaction between the cationic MB and the anionic agaropectin chain of agar. An agar/k-carrageenan composite displayed good dye-adsorption efficiency. A quantity of 242.3 mg/g of dye adsorption was noted using MB as the model dye. Good regeneration capacity is also reported for this hydrogel adsorbent. Moradi et al. [47] demonstrate in their experiment the adsorption performance of chitosan/agar/SiO$_2$ nano hydrogel for pharmaceutical contaminants. Even at a low adsorbent dosage, high removal efficiency (91.15%) for amoxicillin and (99%) for naproxen was noted.

In the light of the above discussion, it is understood that the zeolite, CMC and agar, is a potential candidate for dye-removal process. Hence, the present work aims to prepare a cost-effective and biodegradable membrane using natural polymers such as PVA, CMC and agar. The adsorption properties of the membrane were further improved by incorporating hierarchical zeolite. The biomembrane was tested for Congo red (CR) dye removal from aqueous streams. The biomembrane was characterized using UTM, SEM, TGA, FTIR and other techniques. The adsorption properties of the biomembrane were investigated under various criteria such as altered pH, dye concentration, adsorbent dosage and contact period as well as temperature. The adsorption isotherm and kinetics of the adsorbent was measured. A comparative study of biomembrane with the hierarchical zeolite is also reported.

2. Materials and Methods

2.1. Materials

Tetraethyl orthosilicate (TEOS, 99%), tetrapropylammonium hydroxide (TPAOH, 25% aqueous solution) were procured from Alfa Aesar (Bangalore, India). Aluminum iso-propoxide (AIP) was purchased from Sigma Aldrich (Bangalore, India). Polyvinyl alcohol (PVA) and Congo red (C$_{32}$H$_{22}$N$_6$Na$_2$O$_6$S$_2$) were provided from Ajax Finechem Pvt. Ltd. (Bangkok, Thailand). Glutaraldehyde (GA) and hydrochloric acid (HCl) were obtained from Loba Chemie (Bangkok, Thailand). Carboxymethyl cellulose (CMC) and agar were procured from Chemipan (Bangkok, Thailand). All chemicals were used without any additional purification. The chemical structure, molecular weight and wavelength of maximum absorbance of Congo red is illustrated in Table 1.

Table 1. The molecular structure and properties of Congo red.

Name	MW (g/moL)	Group	λmax (nm)	Structure
Congo red (CR)	696.66	-SO3- -NH2 -N = N-	492	

2.2. Methods

2.2.1. Surfactant Templated ZSM-5 Zeolite Synthesis

Zeolite synthesis was preceded by mixing the aluminium source (aluminium isopropoxide) and structure-directing agent (tetra propylammonium hydroxide) under appropriate conditions [48]. In the next stage, the silica source (tetraethyl orthosilicate) and template (cetyl trimethyl ammonium bromide) are added and stirred to become a homogenous solution. The resulting solution was kept for hydrothermal treatment and heated at 80 °C for 5 days. The product was then brought to room temperature, filtered and washed, followed by drying in an oven at 100 °C for 8 h and lastly the powdered sample was calcinated at 550 °C at a heating rate of 10 °C/min in furnace and later ground with a mortar into fine powder [49].

2.2.2. Preparation of Agar/Zeolite/CMC/PVA Biomembrane

Here, we adopted a simple and eco-friendly solvent-casting method to fabricate a polyvinyl alcohol-agar-carboxymethyl cellulose-zeolite biomembrane. The procedure for the preparation of the biomembrane is as follows. Initially, the required amount of PVA, CMC and agar were dissolved in water under constant stirring. Varied concentrations of zeolite (2 to 6 wt%) were then added to the above mixture and stirred again for few more hours. Later, a crosslinking agent, i.e., GA in HCl, is added and stirred. The crosslinked solutions were cast in a clean glass petri dish with a thickness of 29 μm and dried at room temperature for 3–4 days. The membranes containing 0, 2, 4 and 6 wt% of zeolite were labelled as AG-0, AG-1, AG-2 and AG-3, respectively. The weight percentage of the samples is given in Table 2, as well as a schematic representation of solution-casting method (Scheme 1).

Table 2. The composition of the biomembrane.

| Samples	PVA (wt%)	CMC (wt%)	AGAR (wt%)	ZSM-5 Zeolite (wt%)
AG-0	10	1	4	0
AG-1	10	1	4	2
AG-2	10	1	4	4
AG-3	10	1	4	6

2.3. Characterisation

Thermogravimetric analysis of the prepared samples was undertaken with Mettler Toledo, TGA/DSC 3 + HT/1600 (Greifensee, Switzerland). A required amount of the sample was placed in an aluminium crucible and the mass loss with respect to temperature (50–750 °C) was recorded. The test was carried out under nitrogen atmosphere at a heating rate of 10 °C/min. The dye-adsorption studies were evaluated by a Jasco V-630 UV–VIS spectrophotometer Specord (UV-210, Analytik Jena, Jena, Germany) in the wavelength ranging from 200 to 800 nm. The Fourier transform infrared spectra were identified using a FTIR spectrometer (Invenio S, Bruker, Cambridge, United Kingdom) at 400–4000 cm^{-1}. The surface morphology of agar-carboxymethyl cellulose-zeolite-polyvinyl alcohol biomembrane was evaluated using an optical microscope (Olympus BX43 series, Hamburg, Germany) analyser. The X-ray diffraction pattern of the biomembrane was measured using (Rigaku SmartLab, Raleigh, NC, USA) from 5° to 90° with the monochromatic radiation of CuKα.

The mechanical properties of obtained membranes were evaluated as per the ASTM standard D638-14 using a universal testing machine (UTM) (Cometech QC-508B2, Taichung City, Taiwan). The mechanical test was performed using a rectangular membrane of dimensions 60 mm × 10 mm. The speed of the moving clamp was 10 mm/min, and the gauge length was 50 mm. N$_2$ adsorption isotherms of samples were performed using a Belsorp mini-analyzer (Bochum, Germany). Before the study, the samples were outgassed at 573 K for 4 h in vacuum. The hydrophilic/hydrophobic character of the biomembrane was determined by the contact-angle method using Digidrop (Drop Meter SCA data physics, Stuttgart, Germany). For this, water with a droplet size of 4 μL was placed on the membrane surface. A video of the digidrop recorded the contact angle between the baseline of the waterdrop and the tangent at the drop boundary. The measurements were taken in triplicates and the average contact value is stated. To evaluate the swelling ratio, the biomembrane was cut into equal pieces with dimensions 2 × 2 cm and their initial weight was recorded. The biomembranes were immersed in distilled water at room temperature for 48 h. At a certain time interval, the swollen samples were removed, then gently wiped with filter paper and weighed. The process was repeated until the swollen sample reached a constant weight [50]. The swelling capacity was estimated using Equation (1)

$$\text{Swelling ratio} = \left(\frac{W_s}{W_d} - 1 \right) \tag{1}$$

where W_d and W_s are the weights of dry and wet biomembranes.
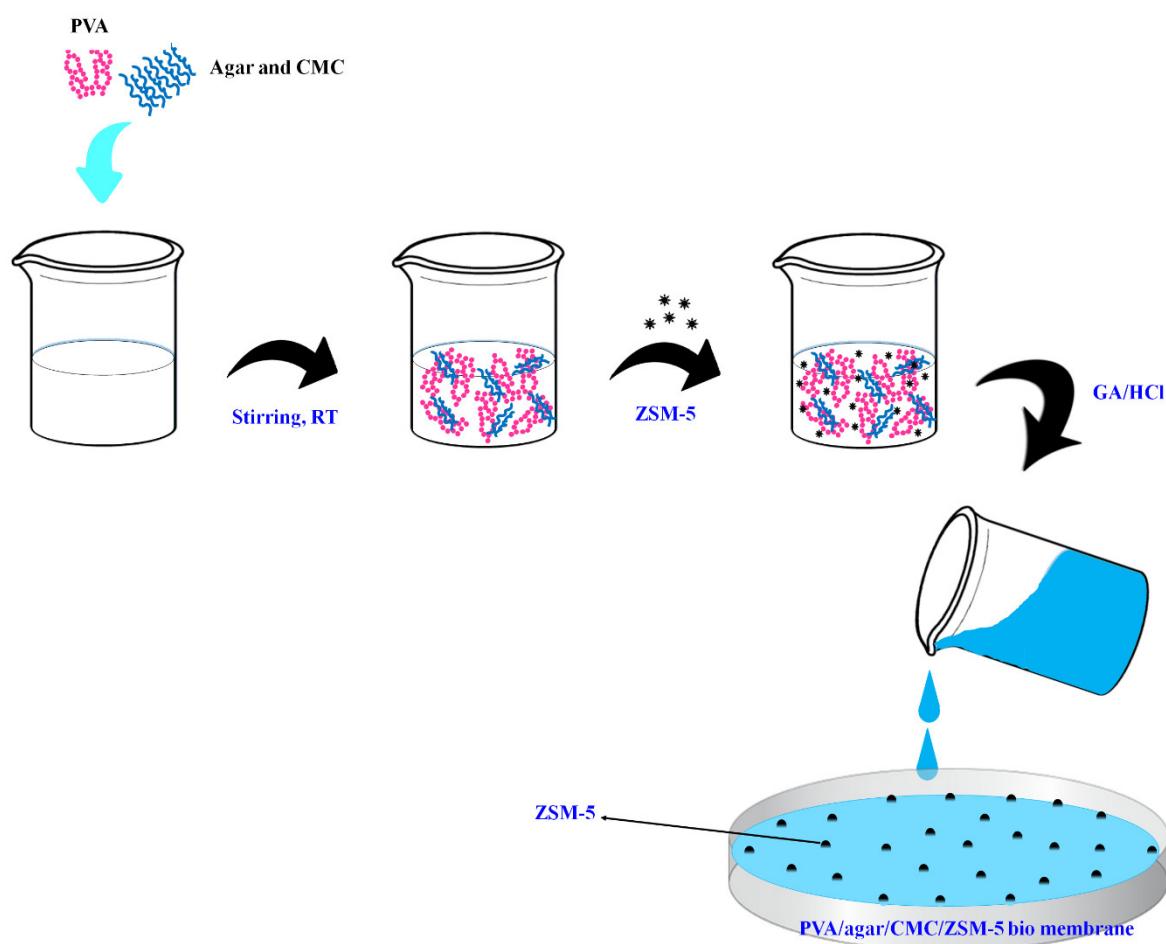
Scheme 1. Schematic representation showing the incorporation of zeolite on the agar/CMC/PVA biomembrane.

Escherichia coli (*E. coli*, Gram negative) and Staphylococcus aureus (*S. aureus*, Gram positive) bacteria were considered to examine the antibacterial property of the biomembranes. Initially the biomembrane was cut into circular shape and seeded on a Mueller Hinton plate Petri B plate inoculated overnight with *E. coli* and *S. aureus* bacteria. The samples were incubated at 37 °C for 18 h. After the incubation period, the zone of inhibition formed around the biomembrane was measured and the diameter of the growth inhibition zone reported [51].

2.4. Adsorption Experiments

The adsorption of CR on agar/zeolite/CMC/PVA biomembrane was carried out by the batch method. Initially, 0.05 g of the agar/zeolite/CMC/PVA biomembrane was immersed in 40 mL of the CR dye solution with constant stirring. The concentration of dye was varied from 20 mgL^{-1} to 100 mgL^{-1}. At certain time intervals, the CR solution was taken out and evaluated using a UV–visible spectrophotometer (Specord (UV-210)) at λ_{max} = 492 nm. The equilibrium adsorption capacity (q_e) and removal percentage (%) was calculated from the equations below.

$$q_e = \frac{(C_0 - C_e)V}{m} \tag{2}$$

$$R(\%) = \frac{C_0 - C_e}{C_0} \times 100 \tag{3}$$

where C_0 is the initial dye concentration (mg L^{-1}) and C_e is the final concentration (mg L^{-1}), respectively; V refers to solution volume (in litres); m is the weight of the biomembrane (in grams).

2.5. Desorption Procedure

The regeneration potential of the biomembranes was performed by successive adsorption/desorption experiments. Initially, 0.05 g of agar/zeolite/CMC/PVA biomembrane was added to the aqueous CR solution (20 mgL^{-1}). After 3 h, the biomembrane was washed with water and mixed with desorbing agent (0.1 N HCl). After desorption, the regenerated adsorbent was taken out and washed extensively with water and oven dried at 70 °C for 8 h for the adsorption tests [52].

3. Result and Discussions

3.1. Characterisation of Agar/Zeolite/CMC/PVA Biomembrane

The porosity of synthesized hierarchical zeolite was examined by nitrogen adsorption isotherm (Figure 1). The synthesised zeolite had a display-type IV isotherm with a broad hysteresis loop from P/P$_0$ = 0.70 to 1. Our result was in accordance with previous reports and indicates the presence of both micro- and mesopores. The BJH pore size distribution of the zeolite further confirms the presence of mesopores in the range of 10–20 nm. The removal of the templating agent from the framework is responsible for the formation of mesoporosity. A similar observation was observed in our previous studies of cellulose-modified ZSM-5 zeolite [49]. The successful addition of filler (zeolite) in the polymer matrix was assessed using XRD, FTIR and morphological analysis. The XRD spectrum of the zeolite and zeolite-loaded biomembranes is presented in Figure 2. Zeolites are known to give diffraction peaks at 2θ = 7.92°, 9.04°, 13.59°, 14.19°, 15.14°, 15.91°, 23.38°, 24.16°, 25.63° and 30.18° attributed to [101], [111], [102], [112], [131], [022], [051], [313], [323] and [062] planes, which is an MFI pentasil structure of ZSM-5 zeolite equivalent to the JCPDS card no. 89-1421. (Figure 2 (inset)) [53]. The presence of the aforementioned peaks in the agar/zeolite/CMC/PVA biomembrane is indicative of the successful dispersion of zeolite in the biomembrane. It is also noted that, on increasing the percentage of zeolite, the peak intensity of the 2θ = 19.4° was reduced. This implies the development of a strong interaction between filler and the polymer [54–56]. We have also calculated the mean crystalline size of the samples using the Debye–Scherrer equation. The average crystalline

of the samples ZSM-5 zeolite, AG-0, AG-1, AG-2 and AG-3 are 19.32, 1.49, 4.17, 7.57 and 10.63 nm, respectively. Meanwhile, the FTIR result shows that the biomembrane displayed major peaks at 3289 cm^{-1} and 2926 cm^{-1} for -OH and -CH stretching; 1730 cm^{-1} for C=O stretching; 1615 cm^{-1} (asymmetric stretching of -COOH), 1420 cm^{-1} (symmetric stretching of -COOH), 1100 cm^{-1}, 835 cm^{-1} and 545 cm^{-1} (symmetrical stretching vibration of Si-O and Al-O bond of zeolite) (Figure 3) [57,58]. Due to the availability of hydroxyl groups, hydrogen-bond interaction is possible between the zeolite and the carboxyl group of CMC and hydroxyl group of agar (Scheme 2). This chemical interaction is reflected in the FTIR spectra (Figure 3b). A major red shift of the main zeolite peak (3450 cm^{-1}) is considered as a strong indication for zeolite and polymer interactions. Chen et al. [59] employed FTIR to comprehend the chemical interactions between the Cr(V) and polypyrole/sugarcane bagasse composite. A shift in the characteristic FTIR adsorption peak of polypyrole/sugarcane bagasse confirms the binding of Cr (VI) with the functional group of the composite. Zhu et al. [60] also observed a shift in peak position on the dye-adsorbed membrane. The authors thus suggested that the mechanism of adsorption is electrostatic in nature. Taken into account the above observation, we compared the FTIR of membrane before and after dye adsorption. It is evident that the peak intensity at 3270 cm^{-1} increased after dye adsorption (Figure 3c). The said peak is the characteristic peak of CR and is associated with the stretching vibration of the -N-H group [61,62]. Meanwhile, the intensity peaks at 2900, 1426, 1215 and 1100 cm^{-1} diminish, and a small red shift was noticed for the characteristic band at 1600 cm^{-1}. The FTIR analysis thus confirms electrostatic attraction between CR and the biomembrane [13]. The adsorption of dye on the biomembrane is further confirmed by UV analysis. The UV spectrum of the biomembrane before and after adsorption is examined and the result is shown in Figure 4a,b. It is obvious from Figure 4a that after dye adsorption, the new peak obtained at 513 nm is the characteristic peak of the CR. The intensity of this characteristic peak increases with an increasing zeolite concentration. Thus, it can be confirmed that a biomembrane loaded with a high concentration of zeolite is a potential adsorbent for CR [34].
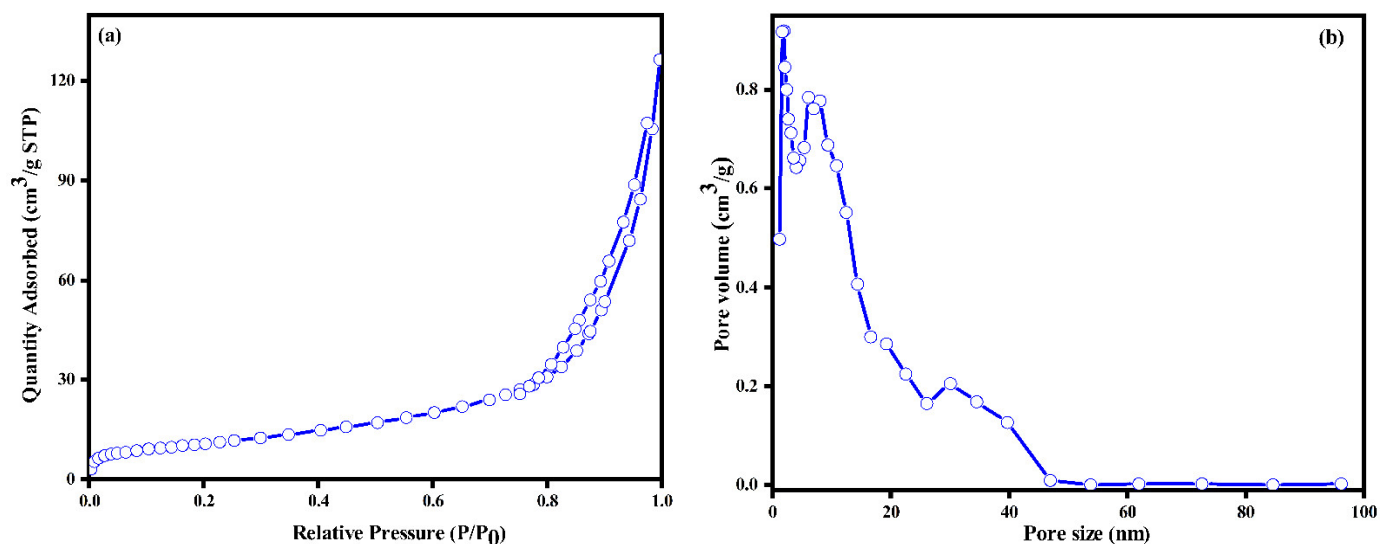

Figure 1. (**a**) Adsorption–desorption isotherm (nitrogen) and (**b**) BJH pore-size distribution of ZSM-5 zeolite.
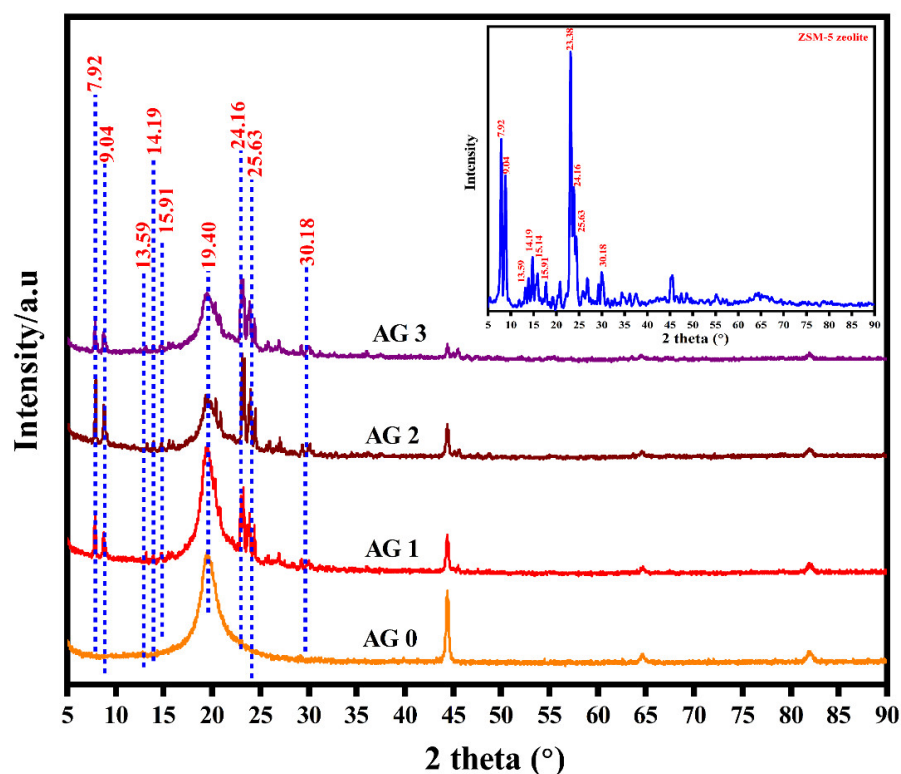
Figure 2. X-ray diffraction (XRD) patterns of zeolite-incorporated agar/cellulose/PVA biomembrane and corresponding ZSM-5 zeolite (inset).

The thermogravimetric and derivative curves of varied-zeolite-percentage loaded agar/CMC/PVA biomembranes are shown in Figure 5. The initial weight loss of 6–13% at 30–170 °C is attributed to the loss of moisture content and other contaminants. The second weight loss starts from 180 to 370 °C, attributed to the degradation of polymers (PVA, CMC and agar) and the final weight loss of 29–34% at 380–650 °C is related to the decomposition of zeolite. [63]. Table 3 summarises the degradation of the polymer at different temperatures. From the table, it is observed that, with an increasing percentage of zeolite content, the amount of degradation decreased from 86.36 to 68.28%. Hence, a zeolite-anchored biomembrane has a high thermally stability, which is desirable for adsorption studies. For comparison the thermogravimetric and differential thermal analysis curves of ZSM-5 zeolite are shown in Supplementary Materials (Figures S1 and S2). The biomembrane was further tested for its mechanical properties and the results obtained from the universal testing machine are displayed in Table 4. Upon incorporation of zeolite, both tensile strength and the elongation at break of the biomembrane decrease. The zeolite particles disturbed the homogeneous structure of the polymer by intermolecular hydrogen bonds, which was confirmed through FTIR analysis [57]. The contact-angle values of the membrane are displayed in Figure 6a. Water contact-angle values increased with zeolite content. Being rich in hydroxyl groups, the agar/CMC/PVA biomembranes have great affinity for water molecules. Therefore, they tend to spread the water droplets and consequently have a high water contact angle (70°). However, with the addition of zeolite, the water-wetting ability of the biomembrane is reduced. This is in accord with the fact that a high-silica zeolite has a low hydrophilic nature and therefore repels water molecules. The water contact angles observed for the 2 wt%, 4 wt% and 6 wt% samples are 73.3°, 78.4° and 89°, respectively [63,64]. The above result is justified by swelling studies. The swelling behaviour of the biomembrane as a function of zeolite content is exhibited in Figure 6b. A pure agar/CMC/PVA biomembrane has a good affinity for water and therefore swells to almost double its initial weight. However, the biomembranes embedded with zeolite have less tendency to attract water molecules and therefore possess a low swelling ratio.

The optical microscopic images of the zeolite-incorporated biomembranes is shown in Figure 7. The photographic images of the inhibition zone formed around the biomembrane are provided as Figure 8. In the absence of zeolite, the biomembrane did not show any antibacterial activity. However, after the addition of zeolite, a small inhibition zone was formed around the membrane. The addition of zeolite increased the total surface area and thereby enhanced the antibacterial activity of the membrane. It can be also noted that maximum zone of inhibition was observed against Gram-positive bacteria. This is due to the difference in the features of Gram-positive and Gram-negative bacteria. Gram-positive bacteria have a single-layered cell wall, while Gram-negative possess a double-layered one. Gram-positive bacteria lack the outer membrane, but a thick outer membrane is present for Gram-negative bacteria. Previous reports showed that the Gram-positive bacteria are quite vulnerable to attack compared to Gram-negative bacteria. Hence, the active components of the agar/zeolite/CMC/PVA membrane can penetrate inside the cell wall of the Gram-positive bacteria, disrupt the cell metabolism and eventually destroy them.
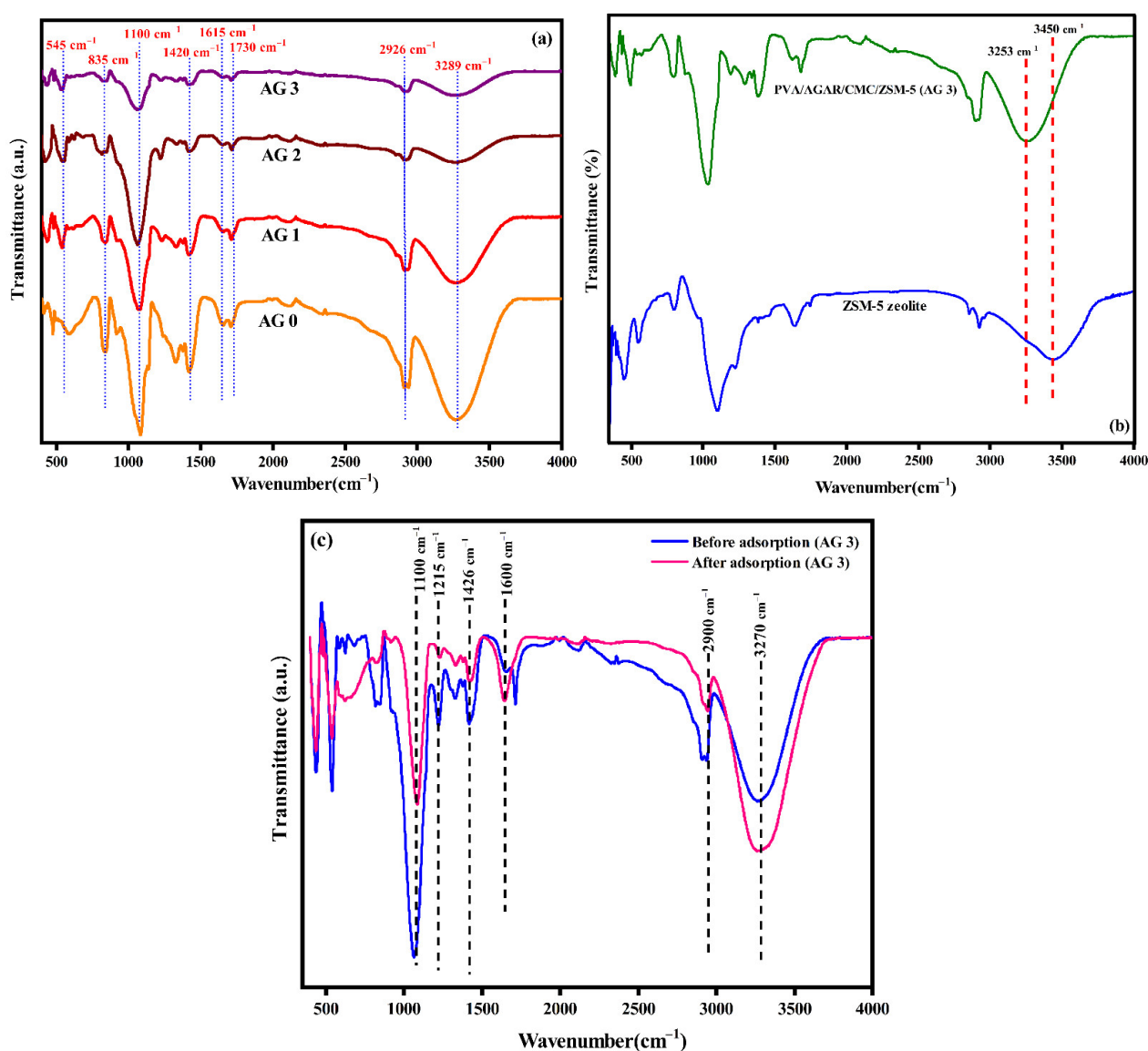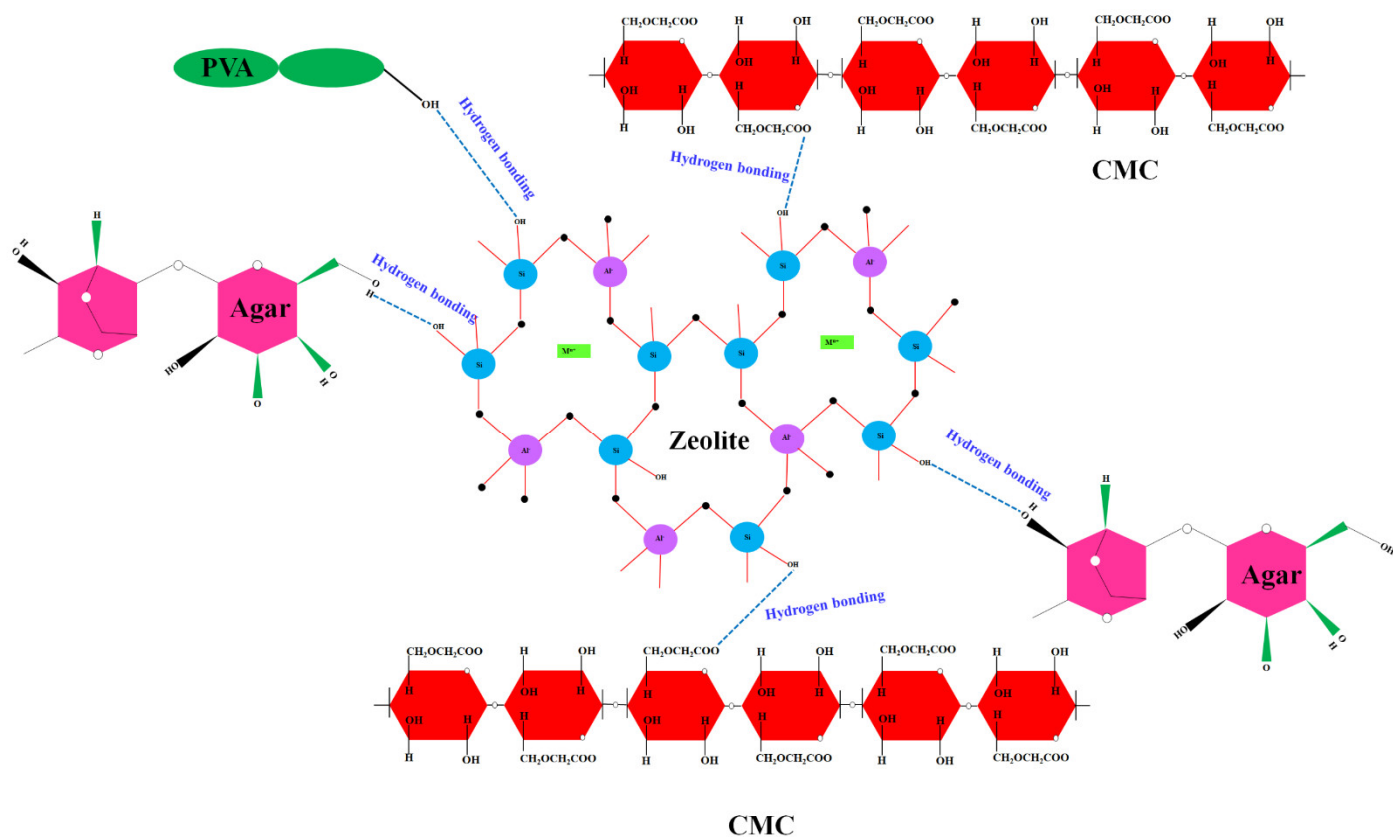

Figure 3. FTIR spectra of: (**a**) agar/CMC/PVA with different percentage of zeolite (**b**) ZSM-5 zeolite and agar/zeolite/CMC/PVA biomembrane (**c**) agar/zeolite/CMC/PVA biomembrane before and after dye adsorption.

Scheme 2. Schematic representation of hydrogen-bond interaction among the hydroxyl groups of zeolite, the carboxyl group of cellulose and the hydroxyl group of agars.
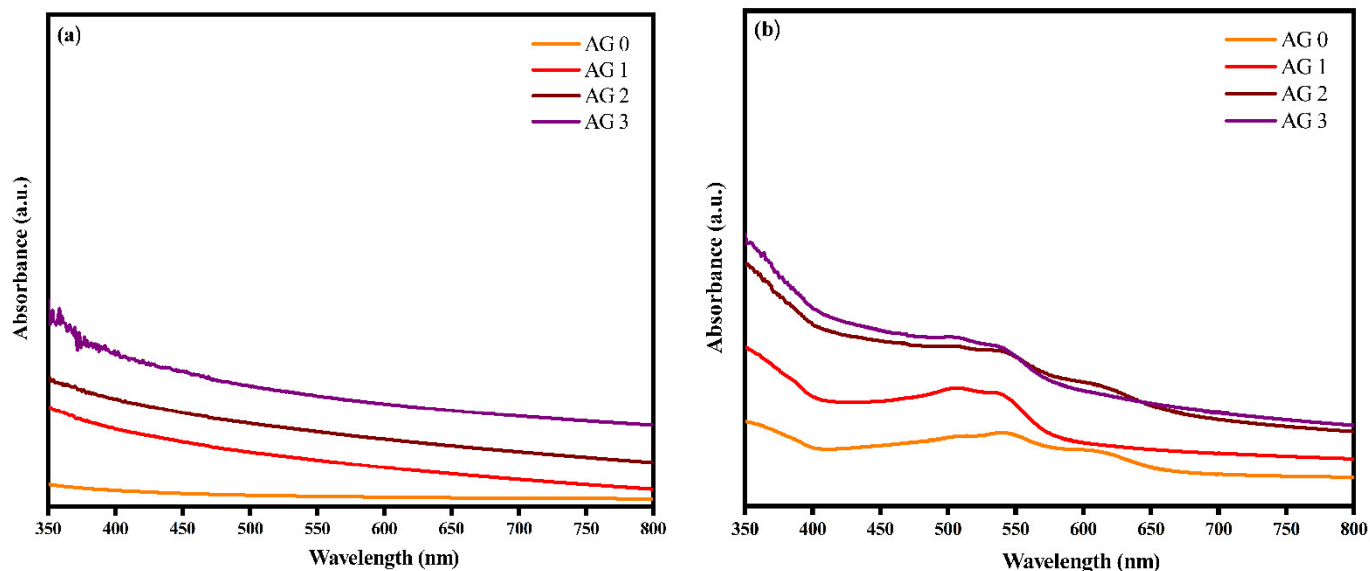

Figure 4. UV–vis spectra of agar/zeolite/CMC/PVA biomembrane: (**a**) before and (**b**) after adsorption of CR.
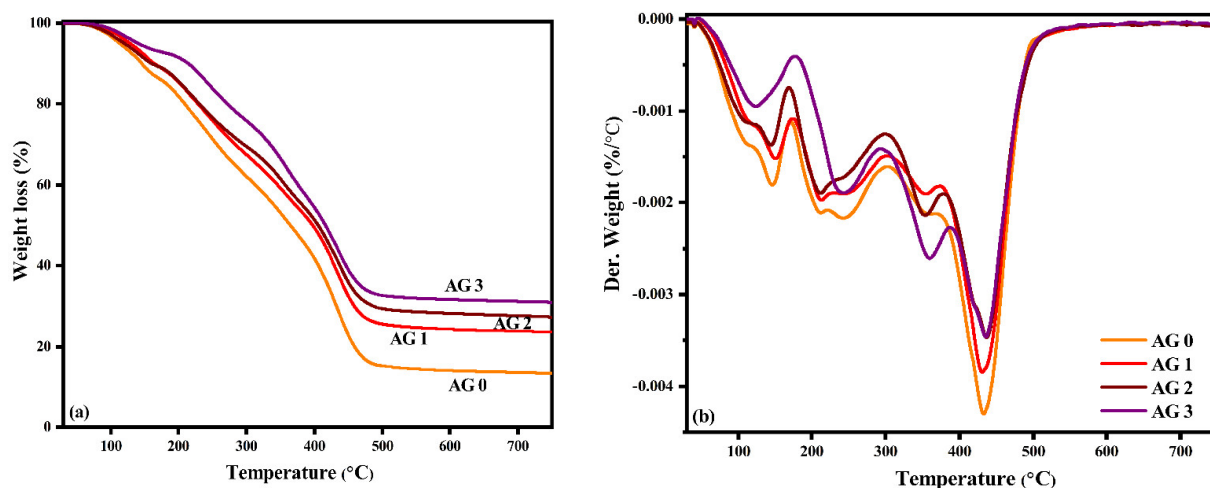
Figure 5. (**a**) Thermogravimetric (TGA) and (**b**) differential thermal analysis (DTA) curves of agar/zeolite/CMC/PVA biomembrane.

Table 3. The result of thermogravimetric results.

Samples Code	Weight Loss of Biomembrane at Different Temperature			Total Weight Loss (%)
	30–170 °C	180–370 °C	380–650 °C	
ZSM-5	9.13	19.56	6.26	34.95
AG-0	13.43	38.07	34.86	86.36
AG-1	10.21	34.61	30.98	75.80
AG-2	10.65	32.14	29.01	71.80
AG-3	6.82	32.05	29.41	68.28

Table 4. Mechanical properties of filler-incorporated systems.

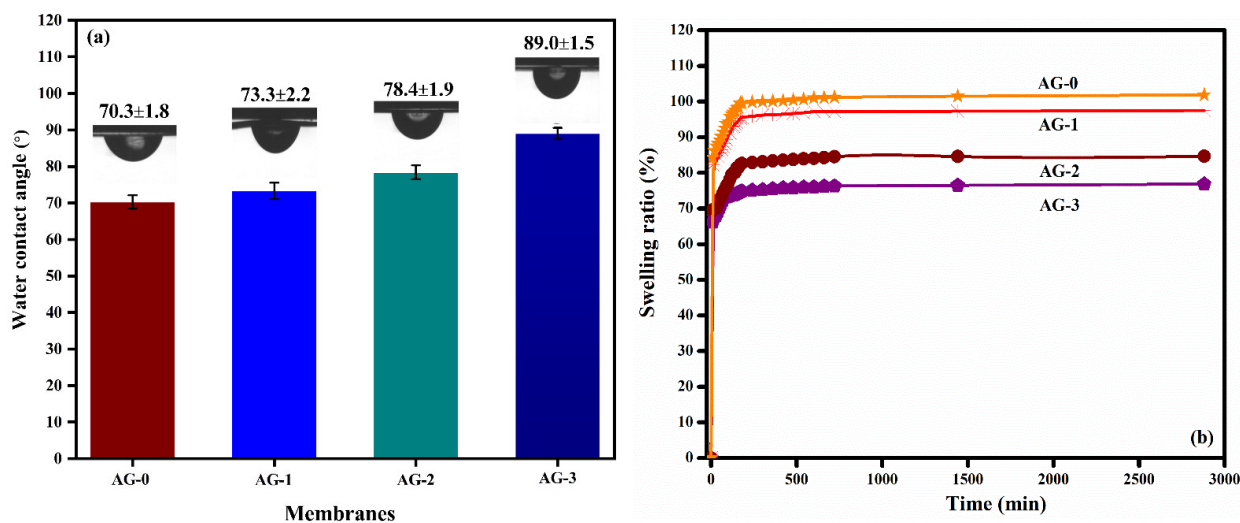| Samples Code	Tensile Strength (MPa)	Elongation at Break (%)
AG-0	35.87 ± 3.35	69.72 ± 3.71
AG-1	31.75 ± 2.40	30.66 ± 5.24
AG-2	29.41 ± 5.04	25.71 ± 3.28
AG-3	23.29 ± 0.46	19.37 ± 4.97

Figure 6. (**a**) Contact angles of droplets on agar/zeolite/CMC/PVA biomembrane and (**b**) swelling ratio with different time intervals of biomembrane based on agar/zeolite/CMC/PVA.
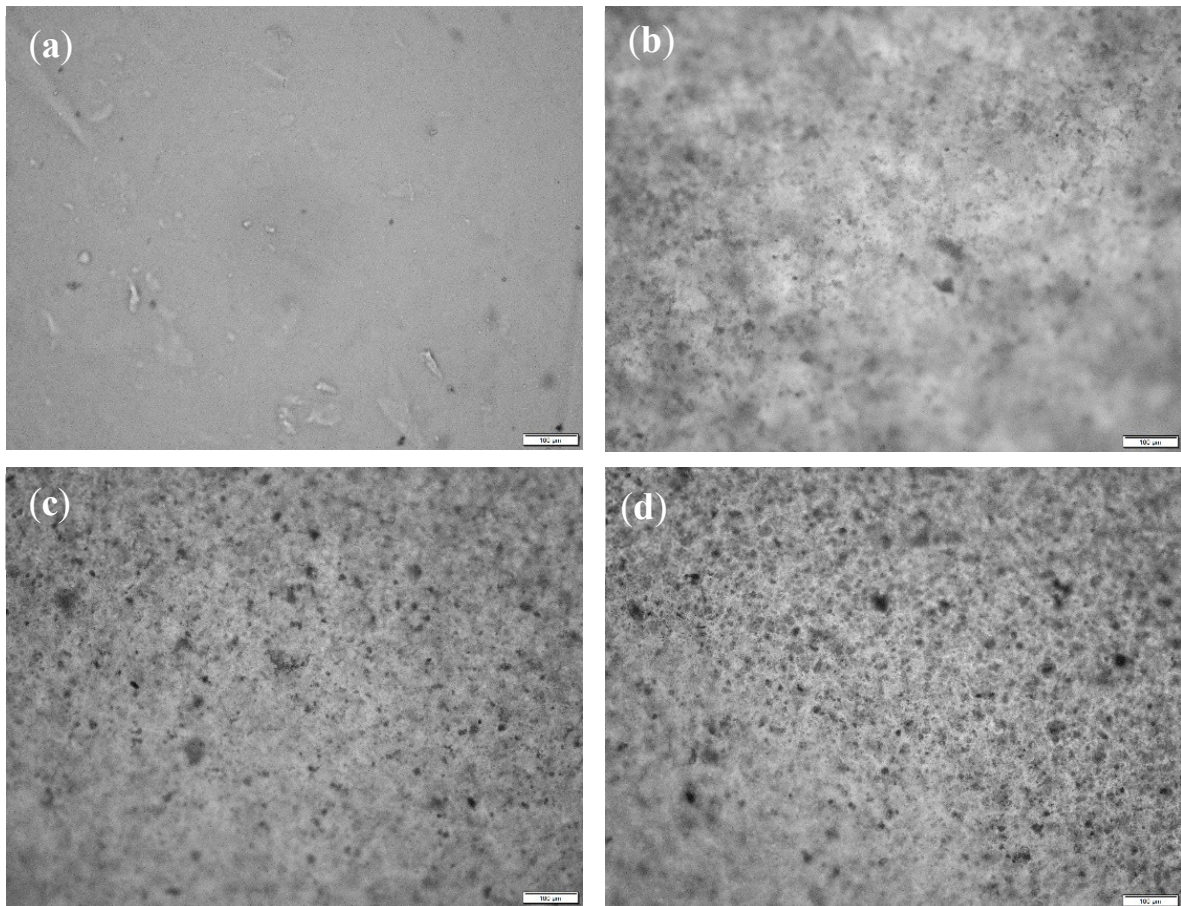
Figure 7. Optical microscopy images of biomembrane: (**a**) AG-0; (**b**) AG 1; (**c**) AG-2; (**d**) AG-3.
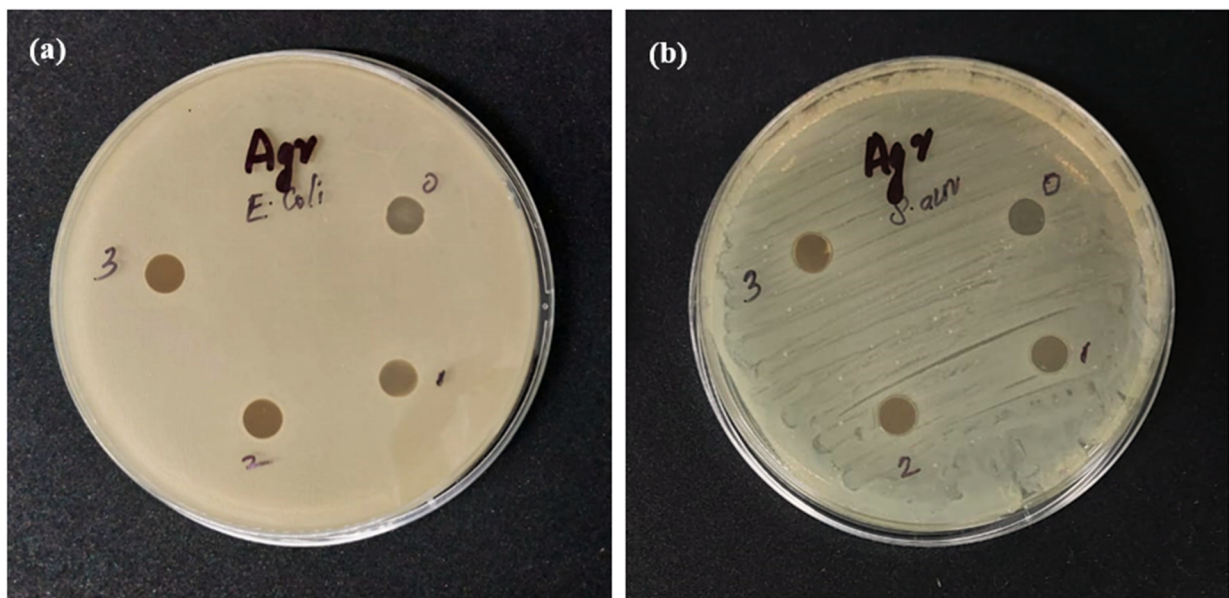

Figure 8. Photograph of antibacterial activity of ZSM-5-loaded biomembrane against (**a**) *E. coli* and (**b**) *S. aureus bacteria*: (0) AG-0; (1) AG-1; (2) AG-2; (3) AG-3.

3.2. Congo Red Removal Performance of Agar/Zeolite/CMC/PVA Biomembrane

Initially, the dye-adsorption efficiency of ZSM-5 was investigated. A quantity of 0.05 g of zeolite was mixed with CR solution and the adsorption capacity was noted at different time intervals. The dye-removal efficiency achieved for ZSM-5 zeolite was only 6.4 mg/g. Therefore, we have systematically studied the consequence of various experimental parameters on the adsorption efficiency of agar/zeolite/CMC/PVA biomembranes. The influence of contact time on the dye-removal efficiency of the membranes was investigated at different time intervals, while keeping all other parameters constant (initial CR concentration of 20 mg/L, 6 wt% dosage, RT) (Figure 9a). In the beginning of the analysis, we could observe a rapid increase in the adsorption rate attributed to the large number of free adsorption sites present on the membrane surface. With the progress of time, the number of free sites on the biomembrane decreased, resulting in a slow rate. The flattening of the curve at a high contact time indicates the saturation point. A similar trend was noted by other researchers for CR adsorption [65,66]. Almost 70% removal efficiency was noted in initially, i.e., 20–30 min. The rapid diffusion of dye molecules and the high surface interaction is responsible for the high removal percentage at the initial contact time. The optimization of the adsorbent dosage is essential for its application purpose. Therefore, in the present study, the adsorption efficiency was assessed at different adsorbent dosages (2 to 6 wt%) (Figure 9b). With increased zeolite content, the active sites on the membrane surface were multiplied and favoured the adsorption process. However, after the optimum concentration was reached (>6 wt%), the surface become saturated with dye molecules and thus the removal percentage did not undergo any enhancement after 6 wt% of zeolite. This is in consonance with the study of Alver et al. [67]. The initial dye concentration highly influences the dye-removal efficiency of the biomembrane. Rida and group [68] mentioned a high adsorption capacity at 40 mg/L methylene blue (MB) concentration. A similar observation was made by Alorabi and group [69]. The effect of C_0 on the adsorption performance of an agar/zeolite/CMC/PVA biomembrane is presented in Figure 9c. The experiment was carried out at 6 wt% adsorbent dosage for a contact time of 3 h at pH = 2. On increasing the CR concentration from 20 mg L^{-1} to 100 mg L^{-1}, the adsorption capacity was also enhanced and reached a maximum value of 64.50 mg/g. The large concentration gradient of dye between the surface and the bulk solution encourages dye adsorption and maximum adsorption capacity was noted when C_0 = 100 mg/L. The pH of the medium influences the adsorbent charge and therefore plays an important role in the adsorption process. The effect of pH on dye adsorption is presented in Figure 9d. In an acidic medium, the adsorbent surface become positive and hence high electrostatic interaction exists between the CR dye molecules and the biomembrane. Meanwhile, in the basic medium, there will be an unfavourable repulsive interaction between CR and the hydroxyl ion due to their negative–negative charges. A similar trend was noted for surfactant-impregnated chitosan beads by Chatterjee et al. [70]. Our result was in compliance with the above reports. From Figure 9d, it is evident that a low pH favours the adsorption of CR on the agar/zeolite/CMC/PVA biomembrane. The influence of temperature on adsorption activity was carried out at an acidic pH (Figure 9e). It is obvious that temperature and CR dye adsorption on the biomembrane are inversely related. A similar trend was reported by Jaseela and group [71] for a mesoporous titania (TiO_2)/polyvinyl alcohol (PVA) nanocomposite system. According to the authors, thermal energy weakens the attraction between the adsorbate and adsorbent which consequently reduces the removal efficiency. The decrease in the adsorption property with higher temperature also indicates the exothermic nature of the adsorbent [72].
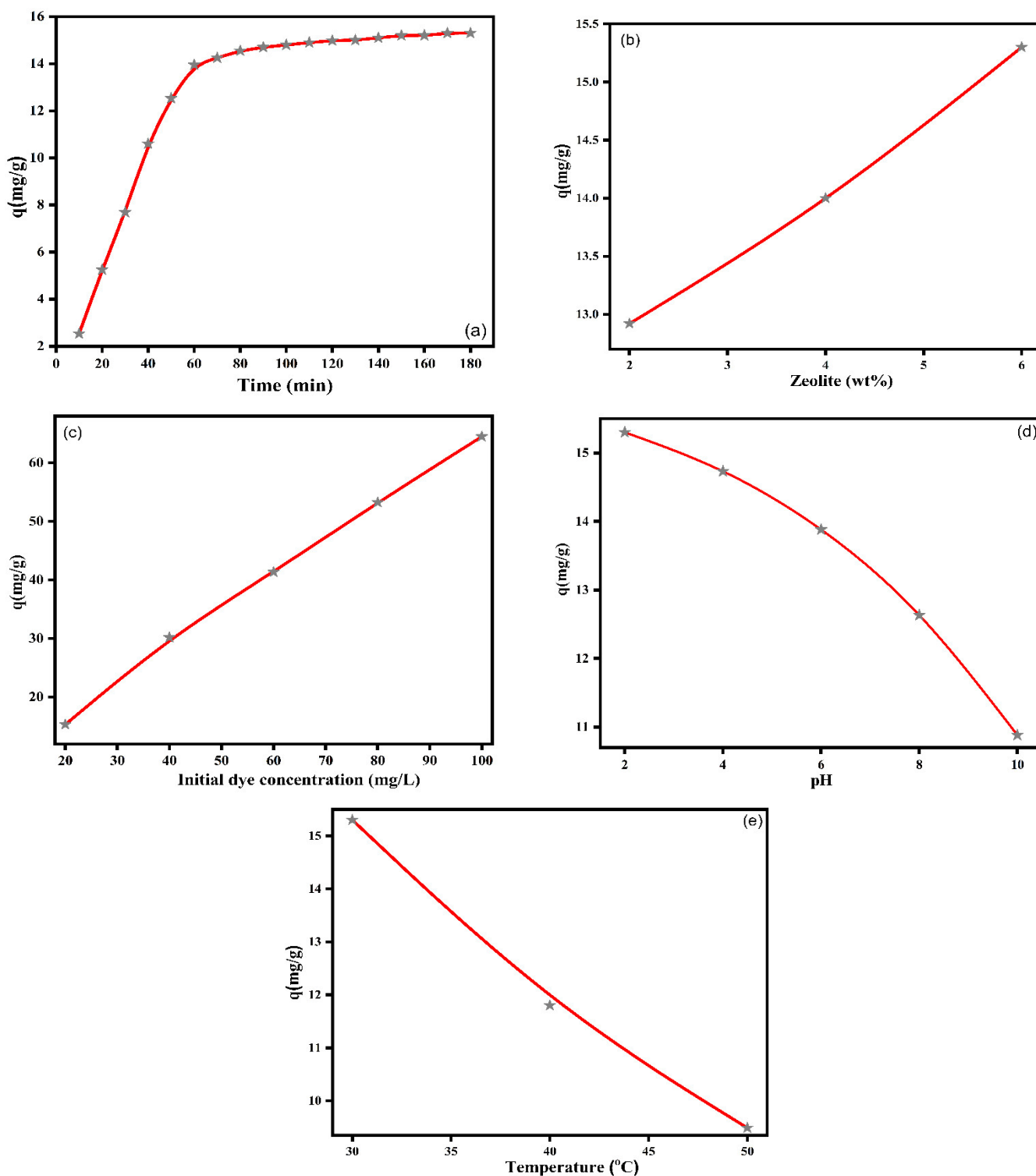
Figure 9. Effect of contact time (**a**), adsorbent loading (**b**), dye concentration (**c**), pH (**d**) and temperature (**e**) on CR uptake capacity (experimental condition: adsorbent dosage 6 wt%, concentration of CR solution 20 mg L^{-1}, pH 2, contact time 3 h and temperature 25 °C).

3.3. Thermodynamics

The thermodynamic study will provide the information about the entropy (ΔS), enthalpy (ΔH) and free energy (ΔG) of the reaction. The negative value of free energy indicates spontaneous adsorption. Meanwhile, positive value suggests non-feasibility of the process [73].

The Gibbs free energy (ΔG) is calculated using the expression

$$\Delta G = -RT \ln K_c \tag{4}$$

where K_c is the adsorption equilibrium constant

$$\Delta G = \Delta H - T\Delta S \tag{5}$$

The values ΔH and ΔS are obtained from the intercept and slope of the plot (ln K_c vs. 1/T) (Van't Hoff), respectively.

The thermodynamics of CR adsorption at three different temperatures, i.e., 303 K, 313 K and 323 K, are displayed in Figure 10 and the obtained parameters are illustrated in Table 5. The negative ΔG (-9.129, -3.16 and -0.49) implied that the CR adsorption process on agar/zeolite/CMC/PVA biomembrane is thermodynamically feasible. Meanwhile, the negative enthalpy (-83.6) confirms that the exothermic nature of adsorption process, and thus complies with the temperature study. The high negative value of entropy implies that the dyes were adsorbed in an orderly fashion on the adsorbate surface. The decrease in randomness at the adsorbent–dye interface has previously been reported by many researchers.
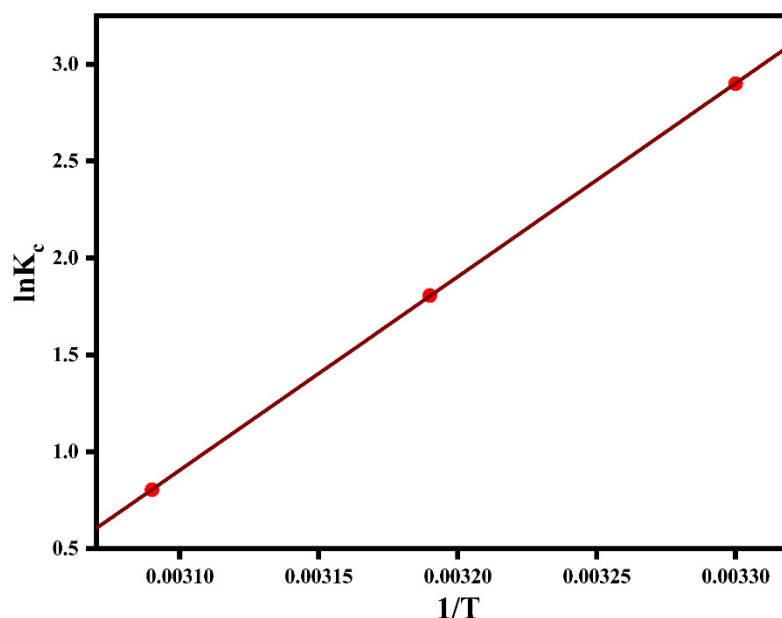

Figure 10. The Van't Hoff plot for CR dye on agar/zeolite/CMC/PVA biomembrane.

Table 5. Thermodynamic parameters for adsorbent agar/zeolite/CMC/PVA biomembrane.

	ΔG(kj/moL)			ΔH(kj/moL)	ΔS (j/moL K)
303 K	313 K	323 K			
-9.129	-3.16	-0.49		-83.6	-257

3.4. Adsorption Kinetics

The adsorption mechanism of CR on the agar/zeolite/CMC/PVA biomembrane was described by pseudo-1st order (PFO), pseudo-2nd order (PSO) and intra-particle diffusion models (IPD) [74–76].

The linearized form of the aforementioned model are stated below.

$$\log(q_e - q_t) = \log q_e - \frac{K_1 t}{2.303} \tag{6}$$

$$\frac{t}{q_e} = \frac{1}{K_2 q_e^2} + \frac{t}{q_e} \tag{7}$$

$$q_t = K_{id}t^{1/2} + C \tag{8}$$

Here, q_t (mg g^{-1}) and q_e (mg g^{-1}) are the adsorption capacity at time 't' and equilibrium, respectively. K_1 and K_2 are the PFO and PSO rate constant which is expressed in min^{-1} and g mg^{-1} min^{-1}. K_{id} is the intraparticle diffusion constant (mg min$^{1/2}$ g^{-1}) while C is the intercept.

The kinetic parameters were calculated from the linear plot of PFO (log ($q_e - q_t$) vs. t), PSO (t/q_t vs. t) and intraparticle diffusion model (q_t vs. $t^{1/2}$) (Figure 11a–c). The kinetic parameters (K_1, K_2 and K_{id}), along with the correlation coefficient, are recorded in Table 6. From Figure 11 and Table 6, it is evident that the experimental value fits better with the PSO model. The correlation coefficients obtained for PFO, PSO and intraparticle diffusion models are 99, 99.5 and 95, respectively. All these results suggest that PSO is more convenient for describing CR adsorption on the agar/zeolite/CMC/PVA biomembrane.
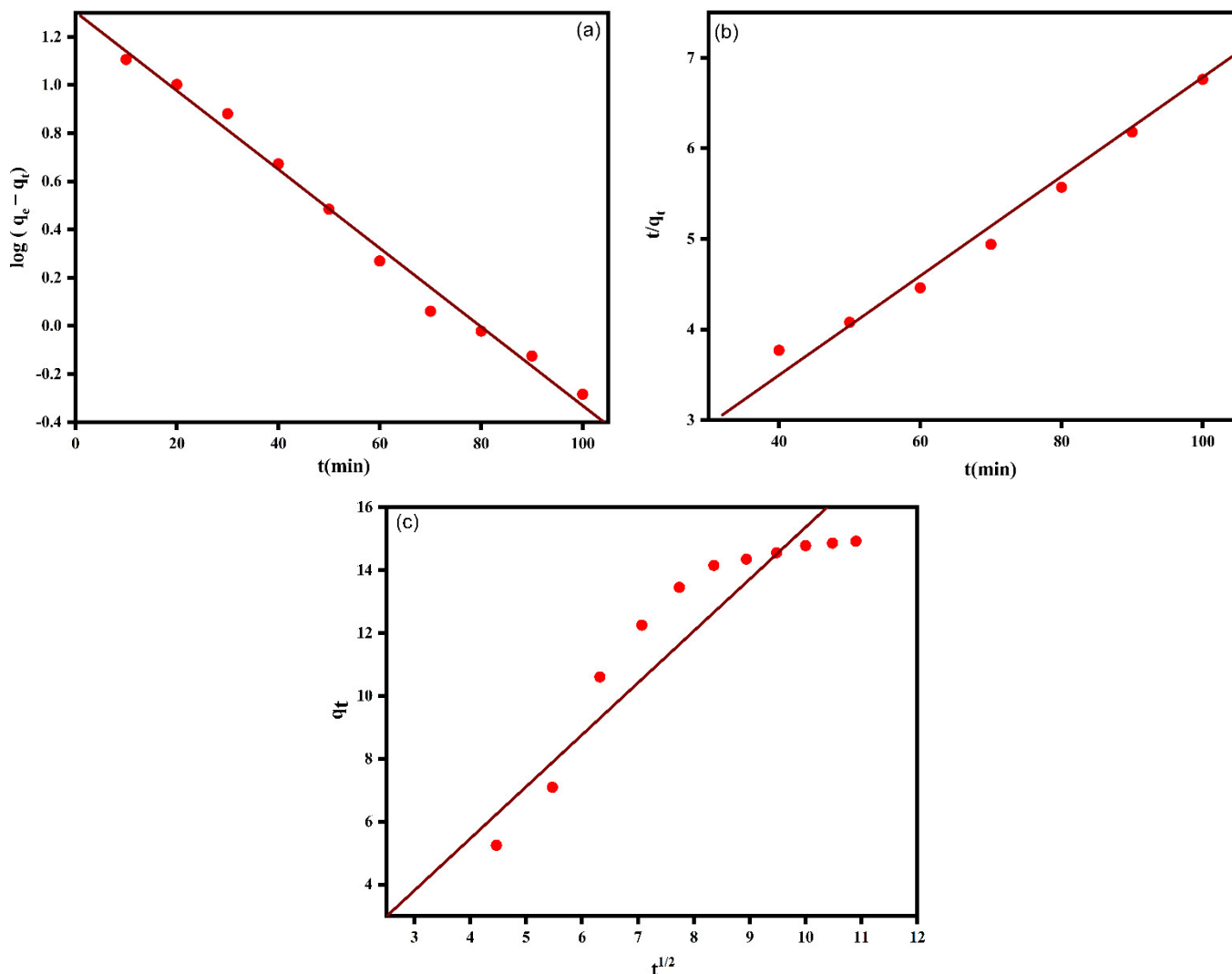

Figure 11. Effect of contact time on (**a**) PFO (**b**) PSO and (**c**) IPD models (adsorbent dosage 6 wt%, concentration of CR solution 20 mg L^{-1}, pH 2, contact time 3 h and temperature 25 °C).

Table 6. Kinetic fitting constants of CR on agar/zeolite/CMC/PVA biomembrane.

Kinetic Models	
PFO	
q_e (mg g^{-1})	3.7
K_L/min	0.0376
R^2	99
PSO	
q_e (mg g^{-1})	18.2
R^2	99.2
K_2 (g mg^{-1} min^{-1})	2.38×10^{-3}
IPD	
C (mg g^{-1})	-1.14
R^2	95
K_{id} (g mg^{-1} min$^{1/2}$)	1.65

3.5. Isothermal Studies

The adsorption isotherm is usually used to identify the adsorption mechanism. The CR equilibrium adsorption on the agar/zeolite/CMC/PVA biomembrane was explained using the Langmuir and Freundlich isotherm model [77,78].

The non-linearized expression of the Langmuir model is expressed as follows.

$$q_e = \frac{q_m K_L C_e}{1 + K_L C_e} \qquad (9)$$

where q_e represents the equilibrium adsorption capacity of the adsorbate (mg g^{-1}), q_{max} (mg g^{-1}) indicates the maximum monolayer adsorption capacity, and C_e is the equilibrium concentration of the adsorbate (mg L^{-1}). K_L represents the Langmuir constant (L mg^{-1}) and is connected to adsorption energy. The linear form of the Langmuir isotherm model is presented in Equation (10).

$$\frac{C_e}{q_e} = \left(\frac{C_e}{q_m}\right) + \left(\frac{1}{K_L * q_m}\right) \qquad (10)$$

The slope and the intercept of the plot of C_e/q_e vs. C_e (Figure 12a) gives the values of q_m and K_L, respectively. Another important parameter is the Langmuir separation factor (R_L), which is mathematically expressed as follows:

$$R_L = \frac{1}{1 + K_L C_0} \qquad (11)$$

The R_L is related to the feasibility and reversibility of the adsorption process. The adsorption process is favourable if R_L comes in the range of zero and one. On the other hand, unfavorable adsorption is noted if the R_L is greater than one.

The linear representation of the Freundlich isotherm is given by

$$\text{In}(q_e) = \text{In}K_F + \frac{1}{n} * \text{In}(C_e) \qquad (12)$$

K_F and n are Freundlich adsorption isotherm constants and are graphically obtained from the linear plot of the Freundlich isotherm (Figure 12b). The value of $1/n$ is used to discover the favourability of the adsorption process. If the $1/n$ value falls under one, it indicates a favourable adsorption. Meanwhile, a value equal to or below zero represents an unfavourable and irreversible adsorption process.
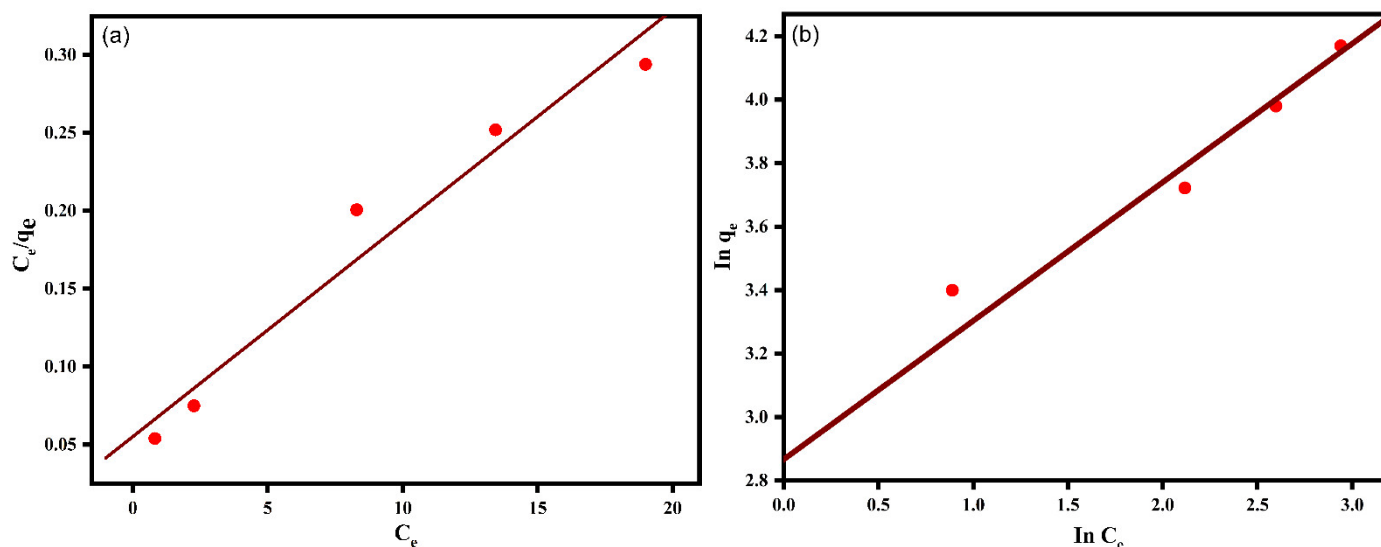
Figure 12. Linear isotherm plots of CR onto agar/zeolite/CMC/PVA biomembrane (**a**) Langmuir (**b**) Freundlich models.

Adsorption isotherm data from experimental studies are corelated with the isotherm curves and the Langmuir and Freundlich models. The fitted parameter along with the correlation coefficient (R^2) is exhibited in Table 7. A good agreement of the experimental adsorption capacity is noted for both models (Langmuir and Freundlich isotherms). The result indicates that both multilayer and monolayer adsorption were involved in the adsorption capacity process.

Table 7. Langmuir and Freundlich isotherm parameters for anionic dye adsorption.

Isotherm Models		
Model	**Parameters**	
Langmuir	q_m (mg g^{-1})	73
	K_L (L mg^{-1})	0.248
	R^2	98
Freundlich	K_F (mg g^{-1})	16.8
	R^2	98
	n	0.436

Scheme of Dye Adsorption

It is evident from FTIR and pH analysis that the surface functional group and its charge plays a major role in dye removal. In addition to this, the zeolite dosage was also found to perform an essential role in CR adsorption on the biomembrane. Our result thus suggests that CR adsorption on the agar/zeolite/CMC/PVA biomembrane is mainly physicochemical in nature. (Scheme 3). The physicochemical nature of dye adsorption is further confirmed by adsorption isotherm and kinetic studies.
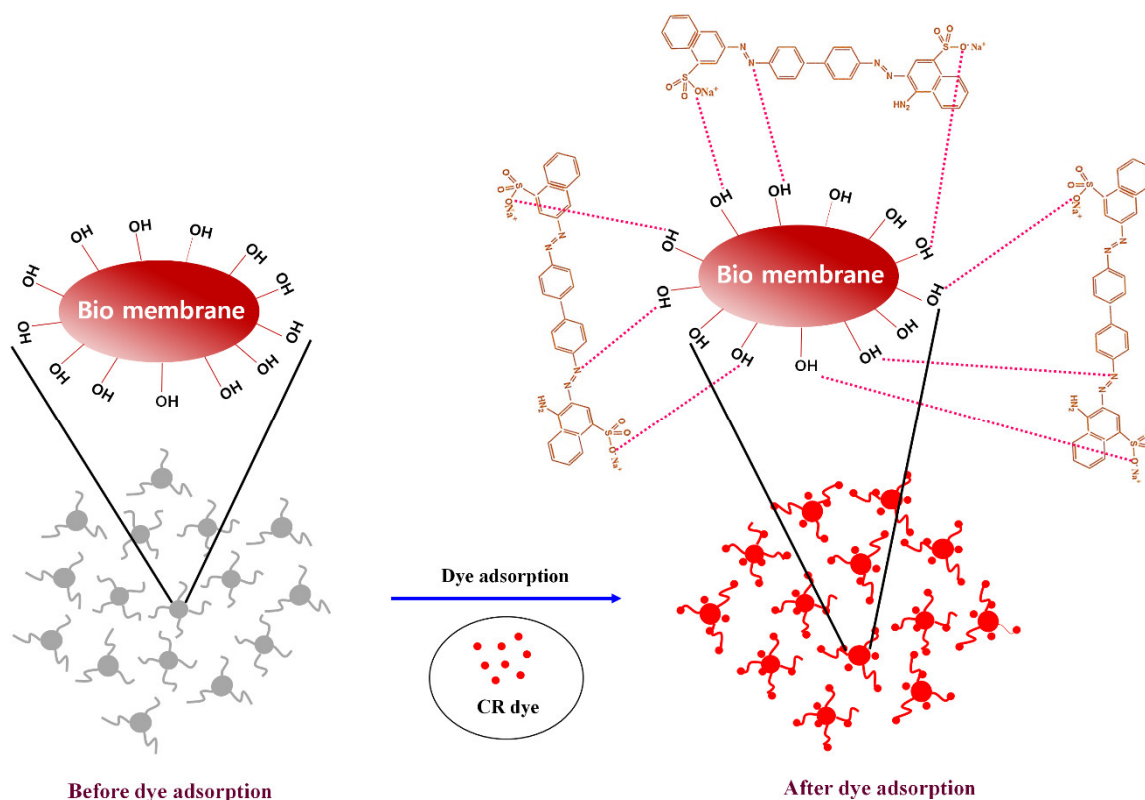
Scheme 3. CR dye molecules interact with the agar/zeolite/CMC/PVA biomembrane.

3.6. Reusability and Regeneration Studies

For industrial application, a proper understanding of reusability of the spent adsorbent is required. The reusability of the agar/zeolite/CMC/PVA biomembrane was conducted using HCl (0.1 N) followed by a water wash. As shown in Figure 13, the removal efficiency of CR is reduced from 95 to 89% in the fifth cycle. The reduction in the adsorption cycle is due to the incomplete removal of dye from the biomembrane, probably due to the formation of robust bonds between the CR molecules and the active sites present on the biomembrane.
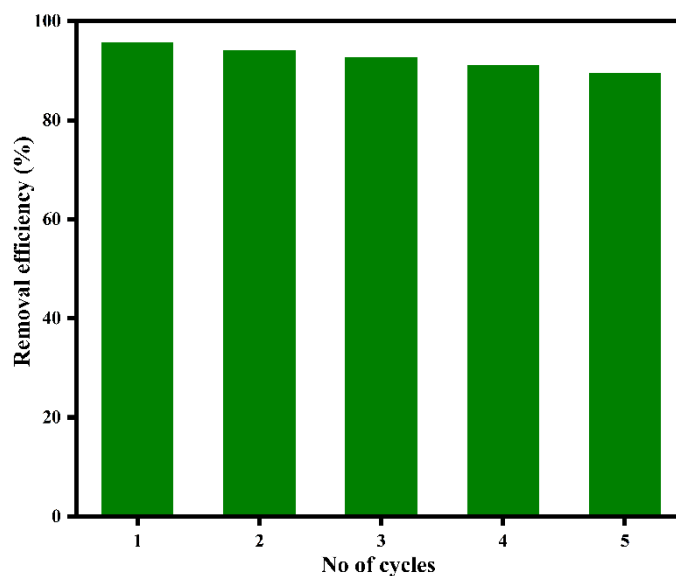

Figure 13. Reusability plot of agar/zeolite/CMC/PVA biomembrane.

3.7. Comparison of Agar/Zeolite/CMC/PVA Biomembrane with Other Adsorbents for CR Adsorption

The adsorption efficiency of the agar/zeolite/CMC/PVA biomembrane is compared with hierarchical zeolite as well as with previously reported adsorbents (Table 8). From the table, it can be noticed that the agar/zeolite/CMC/PVA biomembrane exhibits a higher adsorption capacity than the other reported adsorbents. The high surface area and presence of mesopores in the system is primary factor for the high adsorption property of the biomembrane.

Table 8. Comparison studies of previous work on CR dye on various adsorbents.

Adsorbents	q_e (mg/g)	References
Coir pith carbon	6.7	[76]
Kaolin	5.6	[79]
Zeolite	4.3	[79]
Cabbage waste powder	1.78	[80]
Roots of Eichhornia crassipes	4.81	[81]
Red mud	4.05	[82]
Australian kaolins	5.58	[83]
Bagasse fly ash	11.88	[84]
Rice husk ash	7.047	[85]
Tamarind fruit shell	10.5	[86]
Nilgiri bark	12.4	[87]
Agar/zeolite/CMC/PVA	15.30	This work
ZSM-5 zeolite	6.4	This work

4. Conclusions

In the present study, a carboxymethyl cellulose-agar-polyvinyl alcohol-zeolite biomembrane with efficient adsorption capacity for Congo red is demonstrated. The surface properties of the biomembrane were evaluated using XRD, contact angle, FTIR SEM and TGA analysis. The membrane loaded with 6 wt% of zeolite displayed good thermal stability (68.28% weight loss), high hydrophobicity (89°) and high dye-adsorption performance (96%). The adsorption results revealed that supreme dye-removal efficiency (96%) was achieved at C_o (20 mg/L) with an adsorbent dosage of 6 wt% in an acidic environment (pH 2). The kinetic results showed that the PSO is more fitted than other model with maximum adsorption capacity (18.2 mg/g). The data showed that the adsorption performance of Congo red on carboxymethyl cellulose-agar-polyvinyl alcohol-zeolite biomembrane follows both Langmuir and Freundlich isotherms. The negative free energy (−9.129 KJ/mol) further confirmed the feasibility of the adsorption process. The membrane was also superior in recycling performance. Nearly 90% dye-removal efficiency was noted even after five cycles. Therefore, it can be concluded that the carboxymethyl cellulose-agar-polyvinyl alcohol-zeolite biomembrane is a potential candidate for wastewater management.

Conflicts of Interest: The authors do not have any conflict of interest.

References

1. Qiao, A.; Cui, M.; Huang, R.; Ding, G.; Qi, W.; He, Z.; Klemeš, J.J.; Su, R. Advances in nanocellulose-based materials as adsorbents of heavy metals and dyes. *Carbohydr. Polym.* **2021**, *272*, 118471. [CrossRef]
2. Abou-Zeid, R.E.; Khiari, R.; El-Wakil, N.; Dufresne, A. Current State and New Trends in the Use of Cellulose Nanomaterials for Wastewater Treatment. *Biomacromolecules* **2018**, *20*, 573–597. [CrossRef] [PubMed]
3. Batmaz, R.; Mohammed, N.; Zaman, M.; Minhas, G.; Berry, R.M.; Tam, K.C. Cellulose nanocrystals as promising adsorbents for the removal of cationic dyes. *Cellulose* **2014**, *21*, 1655–1665. [CrossRef]
4. Palma, P.; Alvarenga, P.; Palma, V.L.; Fernandes, R.M.; Soares, A.; Barbosa, I. Assessment of anthropogenic sources of water pollution using multivariate statistical techniques: A case study of the Alqueva's reservoir, Portugal. *Environ. Monit. Assess.* **2009**, *165*, 539–552. [CrossRef] [PubMed]
5. Lee, J.; Chae, H.-R.; Won, Y.J.; Lee, K.; Lee, C.-H.; Lee, H.H.; Kim, I.-C.; Lee, J.-M. Graphene oxide nanoplatelets composite membrane with hydrophilic and antifouling properties for wastewater treatment. *J. Membr. Sci.* **2013**, *448*, 223–230. [CrossRef]
6. Manna, S.; Das, P.; Basak, P.; Sharma, A.K.; Singh, V.K.; Patel, R.K.; Pandey, J.K.; Ashokkumar, V.; Pugazhendhi, A. Separation of pollutants from aqueous solution using nanoclay and its nanocomposites: A review. *Chemosphere* **2021**, *280*, 130961. [CrossRef] [PubMed]
7. Radoor, S.; Karayil, J.; Jayakumar, A.; Parameswaranpillai, J.; Siengchin, S. Efficient removal of methyl orange from aqueous solution using mesoporous ZSM-5 zeolite: Synthesis, kinetics and isotherm studies. *Colloids Surfaces A Physicochem. Eng. Asp.* **2020**, *611*, 125852. [CrossRef]
8. Waheed, A.; Baig, N.; Ullah, N.; Falath, W. Removal of hazardous dyes, toxic metal ions and organic pollutants from wastewater by using porous hyper-cross-linked polymeric materials: A review of recent advances. *J. Environ. Manag.* **2021**, *287*, 112360. [CrossRef]
9. Srivastava, A.; Rani, R.M.; Patle, D.S.; Kumar, S. Emerging bioremediation technologies for the treatment of textile wastewater containing synthetic dyes: A comprehensive review. *J. Chem. Technol. Biotechnol.* **2021**, *97*, 26–41. [CrossRef]
10. Kim, I.; Choi, D.-C.; Lee, J.; Chae, H.-R.; Jang, J.H.; Lee, C.-H.; Park, P.-K.; Won, Y.-J. Preparation and application of patterned hollow-fiber membranes to membrane bioreactor for wastewater treatment. *J. Membr. Sci.* **2015**, *490*, 190–196. [CrossRef]
11. Bilal, M.; Ihsanullah, I.; Younas, M.; Shah, M.U.H. Recent advances in applications of low-cost adsorbents for the removal of heavy metals from water: A critical review. *Sep. Purif. Technol.* **2021**, *278*, 119510. [CrossRef]
12. Gahlot, R.; Taki, K.; Kumar, M. Efficacy of nanoclays as the potential adsorbent for dyes and metal removal from the wastewater: A review. *Environ. Nanotechnol. Monit. Manag.* **2020**, *14*, 100339. [CrossRef]
13. Sabarish, R.; Unnikrishnan, G. Polyvinyl alcohol/carboxymethyl cellulose/ZSM-5 zeolite biocomposite membranes for dye adsorption applications. *Carbohydr. Polym.* **2018**, *199*, 129–140. [CrossRef] [PubMed]
14. Liu, J.; Chen, T.-W.; Yang, Y.-L.; Bai, Z.-C.; Xia, L.-R.; Wang, M.; Lv, X.-L.; Li, L. Removal of heavy metal ions and anionic dyes from aqueous solutions using amide-functionalized cellulose-based adsorbents. *Carbohydr. Polym.* **2020**, *230*, 115619. [CrossRef] [PubMed]
15. Ren, L.; Zhou, D.; Wang, J.; Zhang, T.; Peng, Y.; Chen, G. Biomaterial-based flower-like MnO$_2$@ carbon microspheres for rapid adsorption of amoxicillin from wastewater. *J. Mol. Liq.* **2020**, *309*, 113074. [CrossRef]
16. Siyal, A.A.; Shamsuddin, M.R.; Low, A.; Rabat, N.E. A review on recent developments in the adsorption of surfactants from wastewater. *J. Environ. Manag.* **2019**, *254*, 109797. [CrossRef]
17. Mustafa, R.; Asmatulu, E. Preparation of activated carbon using fruit, paper and clothing wastes for wastewater treatment. *J. Water Process Eng.* **2020**, *35*, 101239. [CrossRef]
18. Svetozarević, M.; Šekuljica, N.; Knežević-Jugović, Z.; Mijin, D. Agricultural waste as a source of peroxidase for wastewater treatment: Insight in kinetics and process parameters optimization for anthraquinone dye removal. *Environ. Technol. Innov.* **2020**, *21*, 101289. [CrossRef]
19. Mahouachi, L.; Rastogi, T.; Palm, W.-U.; Ghorbel-Abid, I.; Chehimi, D.B.H.; Kümmerer, K. Natural clay as a sorbent to remove pharmaceutical micropollutants from wastewater. *Chemosphere* **2020**, *258*, 127213. [CrossRef] [PubMed]
20. Radoor, S.; Karayil, J.; Parameswaranpillai, J.; Siengchin, S. Removal of anionic dye Congo red from aqueous environment using polyvinyl alcohol/sodium alginate/ZSM-5 zeolite membrane. *Sci. Rep.* **2020**, *10*, 15452. [CrossRef]
21. Radoor, S.; Karayil, J.; Parameswaranpillai, J.; Siengchin, S. Adsorption of methylene blue dye from aqueous solution by a novel PVA/CMC/halloysite nanoclay bio composite: Characterization, kinetics, isotherm and antibacterial properties. *J. Environ. Heal. Sci. Eng.* **2020**, *18*, 1311–1327. [CrossRef] [PubMed]

22. Sabarish, R.; Unnikrishnan, G. PVA/PDADMAC/ZSM-5 zeolite hybrid matrix membranes for dye adsorption: Fabrication, characterization, adsorption, kinetics and antimicrobial properties. *J. Environ. Chem. Eng.* **2018**, *6*, 3860–3873. [CrossRef]

23. Zhang, C.-J.; Hu, M.; Ke, Q.-F.; Guo, C.-X.; Guo, Y.-J. Nacre-inspired hydroxyapatite/chitosan layered composites effectively remove lead ions in continuous-flow wastewater. *J. Hazard. Mater.* **2019**, *386*, 121999. [CrossRef] [PubMed]

24. McLeary, E.; Jansen, J.; Kapteijn, F. Zeolite based films, membranes and membrane reactors: Progress and prospects. *Microporous Mesoporous Mater.* **2006**, *90*, 198–220. [CrossRef]

25. Sabarish, R.; Unnikrishnan, G. Synthesis, characterization and evaluations of micro/mesoporous ZSM-5 zeolite using starch as bio template. *SN Appl. Sci.* **2019**, *1*, 989. [CrossRef]

26. Radoor, S.; Karayil, J.; Jayakumar, A.; Parameswaranpillai, J.; Siengchin, S. Removal of Methylene Blue Dye from Aqueous Solution using PDADMAC Modified ZSM-5 Zeolite as a Novel Adsorbent. *J. Polym. Environ.* **2021**, *29*, 3185–3198. [CrossRef]

27. Radoor, S.; Karayil, J.; Jayakumar, A.; Parameswaranpillai, J.; Siengchin, S. An efficient removal of malachite green dye from aqueous environment using ZSM-5 zeolite/polyvinyl alcohol/carboxymethyl cellulose/sodium alginate bio composite. *J. Polym. Environ.* **2021**, *29*, 2126–2139. [CrossRef]

28. Hong, M.; Yu, L.; Wang, Y.; Zhang, J.; Chen, Z.; Dong, L.; Zan, Q.; Li, R. Heavy metal adsorption with zeolites: The role of hierarchical pore architecture. *Chem. Eng. J.* **2018**, *359*, 363–372. [CrossRef]

29. Dong, T.; Liu, W.; Ma, M.; Peng, H.; Yang, S.; Tao, J.; He, C.; Wang, C.; Wu, P.; An, T. Hierarchical zeolite enveloping Pd-CeO₂ nanowires: An efficient adsorption/catalysis bifunctional catalyst for low temperature propane total degradation. *Chem. Eng. J.* **2020**, *393*, 124717. [CrossRef]

30. Dabbawala, A.A.; Ismail, I.; Vaithilingam, B.V.; Polychronopoulou, K.; Singaravel, G.; Morin, S.; Berthod, M.; Al Wahedi, Y. Synthesis of hierarchical porous Zeolite-Y for enhanced CO₂ capture. *Microporous Mesoporous Mater.* **2020**, *303*, 110261. [CrossRef]

31. Radoor, S.; Karayil, J.; Parameswaranpillai, J.; Siengchin, S. Adsorption Study of Anionic Dye, Eriochrome Black T from Aqueous Medium Using Polyvinyl Alcohol/Starch/ZSM-5 Zeolite Membrane. *J. Polym. Environ.* **2020**, *28*, 2631–2643. [CrossRef]

32. Sabarish, R.; Jasila, K.; Aswathy, J.; Jyotishkumar, P.; Suchart, S. Fabrication of PVA/agar/modified ZSM-5 zeolite membrane for removal of anionic dye from aqueous solution. *Int. J. Environ. Sci. Technol.* **2020**, *18*, 2571–2586. [CrossRef]

33. Radoor, S.; Karayil, J.; Jayakumar, A.; Nandi, D.; Parameswaranpillai, J.; Lee, J.; Shivanna, J.M.; Nithya, R.; Siengchin, S. Adsorption of Cationic Dye onto ZSM-5 Zeolite-Based Bio Membrane: Characterizations, Kinetics and Adsorption Isotherm. *J. Polym. Environ.* **2022**, *30*, 3279–3292. [CrossRef]

34. Ismail, A.M.; Menazea, A.A.; Ali, H. Selective adsorption of cationic azo dyes onto zeolite nanorod-based membranes prepared via laser ablation. *J. Mater. Sci. Mater. Electron.* **2021**, *32*, 19352–19367. [CrossRef]

35. Habiba, U.; Afifi, A.M.; Salleh, A.; Ang, B.C. Chitosan/(polyvinyl alcohol)/zeolite electrospun composite nanofibrous membrane for adsorption of Cr⁶⁺, Fe³⁺ and Ni²⁺. *J. Hazard. Mater.* **2017**, *322*, 182–194. [CrossRef] [PubMed]

36. Baheri, B.; Ghahremani, R.; Peydayesh, M.; Shahverdi, M.; Mohammadi, T. Dye removal using 4A-zeolite/polyvinyl alcohol mixed matrix membrane adsorbents: Preparation, characterization, adsorption, kinetics, and thermodynamics. *Res. Chem. Intermed.* **2015**, *42*, 5309–5328. [CrossRef]

37. Jin, X.; Jiang, M.-Q.; Shan, X.-Q.; Pei, Z.-G.; Chen, Z. Adsorption of methylene blue and orange II onto unmodified and surfactant-modified zeolite. *J. Colloid Interface Sci.* **2008**, *328*, 243–247. [CrossRef]

38. Abukhadra, M.R.; Mohamed, A.S. Adsorption Removal of Safranin Dye Contaminants from Water Using Various Types of Natural Zeolite. *Silicon* **2018**, *11*, 1635–1647. [CrossRef]

39. Hamd, A.; Dryaz, A.R.; Shaban, M.; AlMohamadi, H.; Abu Al-Ola, K.A.; Soliman, N.K.; Ahmed, S.A. Fabrication and Application of Zeolite/Acanthophora Spicifera Nanoporous Composite for Adsorption of Congo Red Dye from Wastewater. *Nanomaterials* **2021**, *11*, 2441. [CrossRef]

40. Dryaz, A.R.; Shaban, M.; AlMohamadi, H.; Abu Al-Ola, K.A.; Hamd, A.; Soliman, N.K.; Ahmed, S.A. Design, characterization, and adsorption properties of Padina gymnospora/zeolite nanocomposite for Congo red dye removal from wastewater. *Sci. Rep.* **2021**, *11*, 21058. [CrossRef]

41. Maroofi, S.M.; Mahmoodi, N.M. Zeolitic imidazolate framework-polyvinylpyrrolidone-polyethersulfone composites membranes: From synthesis to the detailed pollutant removal from wastewater using cross flow system. *Colloids Surfaces A Physicochem. Eng. Asp.* **2019**, *572*, 211–220. [CrossRef]

42. Radoor, S.; Karayil, J.; Jayakumar, A.; Parameswaranpillai, J.; Siengchin, S. Release of toxic methylene blue from water by mesoporous silicalite-1: Characterization, kinetics and isotherm studies. *Appl. Water Sci.* **2021**, *11*, 110. [CrossRef]

43. Yu, H.; Hong, H.-J.; Kim, S.M.; Ko, H.C.; Jeong, H.S. Mechanically enhanced graphene oxide/carboxymethyl cellulose nanofibril composite fiber as a scalable adsorbent for heavy metal removal. *Carbohydr. Polym.* **2020**, *240*, 116348. [CrossRef] [PubMed]

44. Mittal, H.; Al Alili, A.; Morajkar, P.P.; Alhassan, S.M. GO crosslinked hydrogel nanocomposites of chitosan/carboxymethyl cellulose—A versatile adsorbent for the treatment of dyes contaminated wastewater. *Int. J. Biol. Macromol.* **2020**, *167*, 1248–1261. [CrossRef]

45. Liu, C.; Omer, A.M.; Ouyang, X.-K. Adsorptive removal of cationic methylene blue dye using carboxymethyl cellulose/k-carrageenan/activated montmorillonite composite beads: Isotherm and kinetic studies. *Int. J. Biol. Macromol.* **2018**, *106*, 823–833. [CrossRef]

46. Varaprasad, K.; Jayaramudu, T.; Sadiku, R. Removal of dye by carboxymethyl cellulose, acrylamide and graphene oxide via a free radical polymerization process. *Carbohydr. Polym.* **2017**, *164*, 186–194. [CrossRef]

47. Moradi, O.; Mhdavi, S.; Sedaghat, S. Synthesis and characterization of chitosan/agar/SiO$_2$ nano hydrogels for removal of amoxicillin and of naproxen from pharmaceutical contaminants. *Res. Sq.* **2021**, 1–23.

48. Sabarish, R.; Unnikrishnan, G. A novel anionic surfactant as template for the development of hierarchical ZSM-5 zeolite and its catalytic performance. *J. Porous Mater.* **2020**, *27*, 691–700. [CrossRef]

49. Sabarish, R.; Unnikrishnan, G. Synthesis, characterization and catalytic activity of hierarchical ZSM-5 templated by carboxymethyl cellulose. *Powder Technol.* **2017**, *320*, 412–419. [CrossRef]

50. Ekici, S.; Işıkver, Y.; Saraydın, D. Poly(Acrylamide-Sepiolite) Composite Hydrogels: Preparation, Swelling and Dye Adsorption Properties. *Polym. Bull.* **2006**, *57*, 231–241. [CrossRef]

51. Darbasizadeh, B.; Fatahi, Y.; Feyzi-barnaji, B.; Arabi, M.; Motasadizadeh, H.; Farhadnejad, H.; Moraffah, F.; Rabiee, N. Crosslinked-polyvinyl alcohol-carboxymethyl cellulose/ZnO nanocomposite fibrous mats containing erythromycin (PVA-CMC/ZnO-EM): Fabrication, characterization and in-vitro release and anti-bacterial properties. *Int. J. Biol. Macromol.* **2019**, *141*, 1137–1146. [CrossRef] [PubMed]

52. Lavanya, C.; Soontarapa, K.; Jyothi, M.S.; Geetha Balakrishna, R. Environmental friendly and cost effective caramel for congo red removal, high flux, and fouling resistance of polysulfone membranes. *Sep. Purif. Technol.* **2019**, *211*, 348–358. [CrossRef]

53. Jesudoss, S.K.; Vijaya, J.J.; Kaviyarasu, K.; Kennedy, L.J.; Ramalingam, R.J.; Al-Lohedan, H.A. Anti-cancer activity of hierarchical ZSM-5 zeolites synthesized from rice-based waste materials. *RSC Adv.* **2017**, *8*, 481–490. [CrossRef]

54. Gupta, S.; Pramanik, A.K.; Kailath, A.; Mishra, T.; Guha, A.; Nayar, S.; Sinha, A. Composition dependent structural modulations in transparent poly(vinyl alcohol) hydrogels. *Colloids Surf. B Biointerfaces* **2009**, *74*, 186–190. [CrossRef] [PubMed]

55. Narayanan, S.; Vijaya, J.J.; Sivasanker, S.; Yang, S.; Kennedy, L.J. Hierarchical ZSM-5 catalyst synthesized by a Triton X-100 assisted hydrothermal method. *Chin. J. Catal.* **2014**, *35*, 1892–1899. [CrossRef]

56. Kittur, A.A.; Kariduraganavar, M.Y.; Toti, U.S.; Ramesh, K.; Aminabhavi, T.M. Pervaporation separation of water-isopropanol mixtures using ZSM-5 zeolite incorporated poly(vinyl alcohol) membranes. *J. Appl. Polym. Sci.* **2003**, *90*, 2441–2448. [CrossRef]

57. Prasad, C.V.; Swamy, B.Y.; Sudhakar, H.; Sobharani, T.; Sudhakar, K.; Subha, M.C.S.; Rao, K.C. Preparation and characterization of 4A zeolite-filled mixed matrix membranes for pervaporation dehydration of isopropyl alcohol. *J. Appl. Polym. Sci.* **2011**, *121*, 1521–1529. [CrossRef]

58. Zhao, Q.; Qian, J.; An, Q.; Gao, C.; Gui, Z.; Jin, H. Synthesis and characterization of soluble chitosan/sodium carboxymethyl cellulose polyelectrolyte complexes and the pervaporation dehydration of their homogeneous membranes. *J. Membr. Sci.* **2009**, *333*, 68–78. [CrossRef]

59. Chen, Z.; Pan, K. Enhanced removal of Cr(VI) via in-situ synergistic reduction and fixation by polypyrrole/sugarcane bagasse composites. *Chemosphere* **2021**, *272*, 129606. [CrossRef]

60. Zhu, Z.; Xiang, M.; Li, P.; Shan, L.; Zhang, P. Surfactant-modified three-dimensional layered double hydroxide for the removal of methyl orange and rhodamine B: Extended investigations in binary dye systems. *J. Solid State Chem.* **2020**, *288*, 121448. [CrossRef]

61. Litefti, K.; Freire, M.S.; Stitou, M.; González-Álvarez, J. Adsorption of an anionic dye (Congo red) from aqueous solutions by pine bark. *Sci. Rep.* **2019**, *9*, 16530. [CrossRef] [PubMed]

62. Acemioğlu, B. Adsorption of Congo red from aqueous solution onto calcium-rich fly ash. *J. Colloid Interface Sci.* **2004**, *274*, 371–379. [CrossRef] [PubMed]

63. Teli, S.B.; Calle, M.; Li, N. Poly(vinyl alcohol)-H-ZSM-5 zeolite mixed matrix membranes for pervaporation separation of methanol–benzene mixture. *J. Membr. Sci.* **2011**, *371*, 171–178. [CrossRef]

64. Prince, J.A.; Singh, G.; Rana, D.; Matsuura, T.; Anbharasi, V.; Shanmugasundaram, T.S. Preparation and characterization of highly hydrophobic poly(vinylidene fluoride)—Clay nanocomposite nanofiber membranes (PVDF–clay NNMs) for desalination using direct contact membrane distillation. *J. Membr. Sci.* **2012**, *397–398*, 80–86. [CrossRef]

65. Madan, S.; Shaw, R.; Tiwari, S.; Tiwari, S.K. Adsorption dynamics of Congo red dye removal using ZnO functionalized high silica zeolitic particles. *Appl. Surf. Sci.* **2019**, *487*, 907–917. [CrossRef]

66. El-Shamy, A.G. An efficient removal of methylene blue dye by adsorption onto carbon dot @ zinc peroxide embedded poly vinyl alcohol (PVA/CZnO$_2$) nano-composite: A novel Reusable adsorbent. *Polymer* **2020**, *202*, 122565. [CrossRef]

67. Alver, E.; Metin, A. Anionic dye removal from aqueous solutions using modified zeolite: Adsorption kinetics and isotherm studies. *Chem. Eng. J.* **2012**, *200–202*, 59–67. [CrossRef]

68. Rida, K.; Bouraoui, S.; Hadnine, S. Adsorption of methylene blue from aqueous solution by kaolin and zeolite. *Appl. Clay Sci.* **2013**, *83–84*, 99–105. [CrossRef]

69. Alorabi, A.Q.; Hassan, M.S.; Azizi, M. Fe$_3$O$_4$-CuO-activated carbon composite as an efficient adsorbent for bromophenol blue dye removal from aqueous solutions. *Arab. J. Chem.* **2020**, *13*, 8080–8091. [CrossRef]

70. Chatterjee, S.; Lee, D.S.; Lee, M.W.; Woo, S.H. Congo red adsorption from aqueous solutions by using chitosan hydrogel beads impregnated with nonionic or anionic surfactant. *Bioresour. Technol.* **2009**, *100*, 3862–3868. [CrossRef]

71. Jaseela, P.; Garvasis, J.; Joseph, A. Selective adsorption of methylene blue (MB) dye from aqueous mixture of MB and methyl orange (MO) using mesoporous titania (TiO$_2$)—Poly vinyl alcohol (PVA) nanocomposite. *J. Mol. Liq.* **2019**, *286*, 110908. [CrossRef]

72. Maleki, A.; Mohammad, M.; Emdadi, Z.; Asim, N.; Azizi, M.; Safaei, J. Adsorbent materials based on a geopolymer paste for dye removal from aqueous solutions. *Arab. J. Chem.* **2018**, *13*, 3017–3025. [CrossRef]

73. Yan, C.; Cheng, Z.; Tian, Y.; Qiu, F.; Chang, H.; Li, S.; Cai, Y.; Quan, X. Adsorption of Ni(II) on detoxified chromite ore processing residue using citrus peel as reductive mediator: Adsorbent preparation, kinetics, isotherm, and thermodynamics analysis. *J. Clean. Prod.* **2021**, *315*, 128209. [CrossRef]

74. Wu, K.-H.; Huang, W.-C.; Hung, W.-C.; Tsai, C.-W. Modified expanded graphite/Fe3O4 composite as an adsorbent of methylene blue: Adsorption kinetics and isotherms. *Mater. Sci. Eng. B* **2021**, *266*, 115068. [CrossRef]

75. Bensalah, H.; Younssi, S.A.; Ouammou, M.; Gurlo, A.; Bekheet, M.F. Azo dye adsorption on an industrial waste-transformed hydroxyapatite adsorbent: Kinetics, isotherms, mechanism and regeneration studies. *J. Environ. Chem. Eng.* **2020**, *8*, 103807. [CrossRef]

76. Hao, L.; Gao, W.; Yan, S.; Niu, M.; Liu, G.; Hao, H. Functionalized diatomite/oyster shell powder doped electrospun polyacrylonitrile submicron fiber as a high-efficiency adsorbent for removing methylene blue from aqueous solution: Thermodynamics, kinetics and isotherms. *J. Mol. Liq.* **2020**, *298*, 112022. [CrossRef]

77. Chen, W.; Ma, H.; Xing, B. Electrospinning of multifunctional cellulose acetate membrane and its adsorption properties for ionic dyes. *Int. J. Biol. Macromol.* **2020**, *158*, 1342–1351. [CrossRef]

78. Bo, L.; Gao, F.; Shuangbao; Bian, Y.; Liu, Z.; Dai, Y. A novel adsorbent Auricularia Auricular for the removal of methylene blue from aqueous solution: Isotherm and kinetics studies. *Environ. Technol. Innov.* **2021**, *23*, 101576. [CrossRef]

79. Vimonses, V.; Lei, S.; Jin, B.; Chow, C.W.K.; Saint, C. Kinetic study and equilibrium isotherm analysis of Congo Red adsorption by clay materials. *Chem. Eng. J.* **2009**, *148*, 354–364. [CrossRef]

80. Wekoye, J.N.; Wanyonyi, W.C.; Wangila, P.T.; Tonui, M.K. Kinetic and equilibrium studies of Congo red dye adsorption on cabbage waste powder. *Environ. Chem. Ecotoxicol.* **2020**, *2*, 24–31. [CrossRef]

81. Wanyonyi, W.C.; Onyari, J.M.; Shiundu, P.M. Adsorption of Congo Red Dye from Aqueous Solutions Using Roots of Eichhornia Crassipes: Kinetic and Equilibrium Studies. *Energy Procedia* **2014**, *50*, 862–869. [CrossRef]

82. Tor, A.; Cengeloglu, Y. Removal of congo red from aqueous solution by adsorption onto acid activated red mud. *J. Hazard. Mater.* **2006**, *138*, 409–415. [CrossRef] [PubMed]

83. Vimonses, V.; Lei, S.; Jin, B.; Chow, C.W.; Saint, C.; Chow, C.; Saint, C. Adsorption of congo red by three Australian kaolins. *Appl. Clay Sci.* **2009**, *43*, 465–472. [CrossRef]

84. Mall, I.D.; Srivastava, V.C.; Agarwal, N.K.; Mishra, I.M. Removal of congo red from aqueous solution by bagasse fly ash and activated carbon: Kinetic study and equilibrium isotherm analyses. *Chemosphere* **2005**, *61*, 492–501. [CrossRef] [PubMed]

85. Chowdhury, A.K.; Sarkar, A.D.; Bandyopadhyay, A. Rice Husk Ash as a Low Cost Adsorbent for the Removal of Methylene Blue and Congo Red in Aqueous Phases. *CLEAN—Soil Air Water* **2009**, *37*, 581–591. [CrossRef]

86. Reddy, M. Removal of Direct Dye from Aqueous Solutions with an Adsorbent Made from Tamarind Fruit Shell, an Agricultural Solid Waste. *J. Sci. Ind. Res.* **2006**, *65*, 443–446.

87. Meshram, E.; Meshram, S. Evaluation of adsorptive capacity of bioadsorbent in removal of Congo Red from aqueous solution, Inst. *J. Res. Sci.* **2015**, *4*, 2217–2221.